

Nanopolysaccharide coatings for functional surfaces in water-treatment materials

From mechanisms to process scalability

Andrea Aguilar Sánchez



Nanopolysaccharide coatings for functional surfaces in water-treatment materials

From mechanisms to process scalability

Andrea Aguilar Sánchez

Academic dissertation for the Degree of Doctor of Philosophy in Materials Chemistry at Stockholm University to be publicly defended on Friday 6 May 2022 at 13.00 in Magnélisalen, Kemiska övningslaboratoriet, Svante Arrhenius väg 16 B and online via Zoom, public link is available at the department website.

Abstract

In this thesis, materials from renewable resources were used to develop functionalized surfaces for water treatment. The work is thus inspired by, and contributes to, the United Nations sustainable goals of: (i) clean water and sanitation, (ii) climate action, (iii) responsible consumption and production, (iv) life below water, and (v) partnerships for the goals.

Nanopolysaccharides, most specifically nanocellulose and nanochitin, are great candidates for functional and renewable materials for multiple applications, including the treatment of water and wastewater. This thesis focused on the formulation of different types of nanopolysaccharide-based coatings to enhance the performance of commercially available membranes and cellulose fabrics. We developed a simple waterborne layer-by-layer cellulose nanocrystals (CNC) and TEMPO-oxidized cellulose nanofibrils (T-CNF) coating for commercially available membranes. By changing the surface and pore structure of the membrane, the coating tuned which substrates could pass through the membrane, improved antifouling performance, and when derived from T-CNF, it was harmful to bacterial colonization. Considering the observed T-CNF's effect on bacteria, we developed a chemically crosslinked T-CNF/Poly(vinyl) alcohol (PVA) coating with outstanding antibiofouling performance, ion adsorption/rejection combined with size exclusion, and with dimensional and pH stability. Furthermore, we used a surface-impregnation approach based on bio-based nanotechnology which resulted in highly efficient, with improved mechanical properties, and fully bio-based high-flux water filtration membranes using commercially available nonwoven fabrics. Membranes with coatings prepared from CNC, chitin nanocrystals (ChNC) and T-CNF separated particles in the size range of bacteria and viruses, and those prepared from also T-CNF showed high microplastic filtration efficiency. Moreover, membrane coating based on ChNC and T-CNF had outstanding antibacterial properties.

Overall, we demonstrated that nanopolysaccharide coatings on membranes could provide a significant reduction in organic fouling and biofilm formation while enabling the adsorption of ions and separation of microplastics. In the case of biofilm formation, the functional group and surface charge of the different nanopolysaccharides determined the effect over bacteria, indicating that surfaces could be tailored against microbes. In addition, we directly compared the effect of the different nanopolysaccharides of interest (CNC, T-CNF, ligno-celullose nanocrystals (L-CNC), and ChNC) on bacterial viability and biofilm formation, and found a great difference between the different types of nanocellulose and a different mechanism for nanochitin. Thorough, none of the nanopolysaccharides displayed cytotoxic effects while in indirect contact with the bacterial cells. Nevertheless, T-CNF, ChNC and L-CNC showed a cytostatic effect on bacterial proliferation. Furthermore, the nanomechanical properties of the bacterial cells and interacting forces between the nanopolysaccharides and *Escherichia coli* (*E. coli*) were affected when in direct contact with the nanopolysaccharide surfaces.

Lastly, we upscaled one of our coating processes, demonstrating that the method could be easily implemented at an industrial level. The impact of this thesis relies on the effectiveness of the coatings, the different types of functionalities observed, the demonstrated fast implementation at an industrial scale, and the potential to extrapolate this technology to other applications.

Keywords: *nanopolysaccharides, coating, water treatment, nanocellulose, nanochitin, antifouling, antibacterial, separation technologies.*

Stockholm 2022

<http://urn.kb.se/resolve?urn=urn:nbn:se:su:diva-203187>

ISBN 978-91-7911-838-9
ISBN 978-91-7911-839-6

**Department of Materials and Environmental
Chemistry (MMK)**

Stockholm University, 106 91 Stockholm



**Stockholm
University**

NANOPOLYSACCHARIDE COATINGS FOR FUNCTIONAL
SURFACES IN WATER-TREATMENT MATERIALS

Andrea Aguilar Sánchez

Nanopolysaccharide coatings for functional surfaces in water-treatment materials

From mechanisms to process scalability

Andrea Aguilar Sánchez

©Andrea Aguilar Sánchez, Stockholm University 2022

ISBN print 978-91-7911-838-9

ISBN PDF 978-91-7911-839-6

Printed in Sweden by Universitetsservice US-AB, Stockholm 2022

To Kika, who taught me
how to laugh at life, even
when the sun stops
shining & that the world
is way too big to see only
a corner of it. (Gloria
Castro Pérez,
09-04-44/23-09-19)
& to my mother, for her
infinite love.

“If your dreams don't scare you, they are not big enough.”

- Ellen Johnson Sirleaf, Nobel Peace Prize 2011

“Life is long, and you can have many different lives. You can learn many different things, and you never know when they will be useful, so learn as much as you can and combine your knowledge in new ways. Adapt, be flexible and never stop learning.”

-Frances H. Arnold, Nobel Prize in Chemistry 2018

Abstract

In this thesis, materials from renewable resources were used to develop functionalized surfaces for water treatment. The work is thus inspired by, and contributes to, the United Nations sustainable goals of: (i) clean water and sanitation, (ii) climate action, (iii) responsible consumption and production, (iv) life below water, and (v) partnerships for the goals.

Nanopolysaccharides, most specifically nanocellulose and nanochitin, are great candidates for functional and renewable materials for multiple applications, including the treatment of water and wastewater. This thesis focused on the formulation of different types of nanopolysaccharide-based coatings to enhance the performance of commercially available membranes and cellulose fabrics. We developed a simple waterborne layer-by-layer cellulose nanocrystals (CNC) and TEMPO-oxidized cellulose nanofibrils (T-CNF) coating for commercially available membranes. By changing the surface and pore structure of the membrane, the coating tuned which substrates could pass through the membrane, improved antifouling performance, and when derived from T-CNF, it was harmful to bacterial colonization. Considering the observed T-CNF's effect on bacteria, we developed a chemically crosslinked T-CNF/Poly(vinyl) alcohol (PVA) coating with outstanding antibiofouling performance, ion adsorption/rejection combined with size exclusion, and with dimensional and pH stability. Furthermore, we used a surface-impregnation approach based on bio-based nanotechnology which resulted in highly efficient, with improved mechanical properties, and fully bio-based high-flux water filtration membranes using commercially available nonwoven fabrics. Membranes with coatings prepared from CNC, chitin nanocrystals (ChNC) and T-CNF separated particles in the size range of bacteria and viruses, and those prepared from also T-CNF showed high microplastic filtration efficiency. Moreover, membrane coating based on ChNC and T-CNF had outstanding antibacterial properties.

Overall, we demonstrated that nanopolysaccharide coatings on membranes could provide a significant reduction in organic fouling and biofilm formation while enabling the adsorption of ions and separation of microplastics. In the case of biofilm formation, the functional group and surface charge of the different nanopolysaccharides determined the effect over bacteria, indicating that surfaces could be tailored against microbes. In addition, we directly compared the effect of the different nanopolysaccharides of interest (CNC, T-CNF, ligno-celullose nanocrystals (L-CNC), and ChNC) on bacterial viability and biofilm formation, and found a great difference between the different types of nanocellulose and a different mechanism for nanochitin. Thorough,

none of the nanopolysaccharides displayed cytotoxic effects while in indirect contact with the bacterial cells. Nevertheless, T-CNF, ChNC and L-CNC showed a cytostatic effect on bacterial proliferation. Furthermore, the nanomechanical properties of the bacterial cells and interacting forces between the nanopolysaccharides and *Escherichia coli* (*E. coli*) were affected when in direct contact with the nanopolysaccharide surfaces.

Lastly, we upscaled one of our coating processes, demonstrating that the method could be easily implemented at an industrial level. The impact of this thesis relies on the effectiveness of the coatings, the different types of functionalities observed, the demonstrated fast implementation at an industrial scale, and the potential to extrapolate this technology to other applications.

Sammanfattning

I den här avhandlingen har material från förnybara resurser använts för att utveckla funktionaliserade ytor för vattenrening. Arbetet är därmed inspirerat från, och bidrar till, Förenta Nationernas globala mål för hållbar utveckling; (i) rent vatten och sanitet för alla, (ii) bekämpa klimatförändringarna, (iii) hållbar konsumtion och produktion, (iv) hav och marina resurser och (v) genomförande och globalt partnerskap.

Nanopolysackarider, närmare bestämt nanocellulosa och nanokitin, är utmärkta kandidater som funktionella och förnybara material för en mängd olika användningsområden, bland annat rening av dricks- och avfallsvatten. Vi har fokuserat på att tillverka olika typer av nanopolysackaridbaserade ytbeläggningar för att förbättra kommersiellt tillgängliga membran och cellulosa material. Vi har utvecklat enkla, vattenburna lager-på-lager cellulosanokristaller (CNC) och TEMPO-oxiderade nanofibriller (T-CNF) som ytbeläggningar för kommersiellt tillgängliga membran. Genom att ändra ytan och porstrukturen av membranen kunde ytbeläggningarna användas för att finjustera avskiljningsgraden av särskilda substanser och förbättra anti-fouling egenskaperna hos membranen. Dessutom uppvisade T-CNF beläggningen en nedbrytande effekt mot bakterier. Med denna antibakteriella effekt i åtanke utvecklade vi en kemiskt korslänkad T-CNF/Poly(vinyl)alkohol (PVA) ytbeläggning med enastående anti-fouling prestanda, jon adsorption/avskiljning kombinerad med storleksseparation samt med dimensions- och pH-stabilitet. Utöver detta använde vi en ytimpregneringsmetod baserad på bionanoteknologi, vilket resulterade i en mycket effektiv och helt bio-baserad högflödesvattenfiltreringsmembran baserad på kommersiellt tillgängliga nonwoven material. Detta förbättrade de mekaniska egenskaperna av materialet, där T-CNF beläggningen visade stor potential för filtrering av mikroplaster medan CNC, ChNC samt T-CNF beläggningarna visade god separation av partiklar i storleksordning av bakterier och virus. T-CNF och ChNC beläggningarna visade även enastående antibakteriella egenskaper.

Allt som allt har vi visat att nanopolysackaridbaserade ytbeläggningar på membran kunde bidra till en avsevärd minskning av organisk fouling och biofilmbildning och samtidigt möjliggöra för adsorption av joner och separering av mikroplaster. De funktionella grupperna och ytladdningen av de olika polysackariderna var avgörande för den antibakteriella effekten, vilket visar på att ytbeläggningarna kan skraddarsys mot mikrober. Slutligen jämförde vi effekten mellan de olika polysackariderna i fråga (CNC, T-CNF, L-CNC and ChNC) gällande bakteriell livsduglighet och biofilmbildning,

vilket visade en betydande skillnad mellan de olika typerna av nanocellulosa och en annorlunda mekanism för nanokitin. Sammantaget visade ingen av nanopolysackariderna cytotoxiska effekter, även om T-CNF, ChNC och L-CNC hade en cytostatisk effekt på bakteriell cellförökning.

Till sist har vi framgångsrikt skalat upp en av våra ytbeläggningsprocesser och därmed demonstrerat att metoden enkelt kan implementeras på industriell nivå. Inverkan av denna avhandling kommer av effektiviteten av de presenterade ytbeläggningarna, den påvisade snabba implementeringen i industriell skala och möjligheten att applicera denna teknologi inom andra tillämpningsområden.

Resumen

A lo largo de los estudios presentados en esta tesis, materiales provenientes de recursos renovables fueron utilizados para desarrollar superficies funcionales para tratamiento de agua. Este trabajo fue inspirado por y contribuye a los objetivos globales para el desarrollo sostenible propuestos por las Naciones Unidas; (i) agua limpia y saneamiento, (ii) acción por el clima, (iii) producción y consumo responsables, (iv) vida submarina, y (v) alianzas para lograr los objetivos.

Los nanopolisacáridos, más específicamente la nanocelulosa y la nanoquitina, son excelentes candidatos para ser utilizados como materiales funcionales para múltiples aplicaciones, como en las tecnologías de tratamiento de agua y aguas residuales; además de ser de origen renovable.

Esta tesis se centró en la formulación de diferentes tipos de recubrimientos a base de nanopolisacáridos para mejorar el rendimiento de membranas y textiles de celulosa disponibles comercialmente. Desarrollamos un recubrimiento simple de nanocristales de celulosa (CNC) y nanofibras de celulosa oxidada (T-CNF), utilizando agua como solvente y por medio de la técnica capa-por-capas, para ser usado en membranas comerciales.

Al cambiar la superficie y la estructura de los poros de la membrana, el recubrimiento afinó qué sustratos podían atravesar la membrana y mejoró las propiedades antiincrustantes. Además, se observó que cuando se derivaba de T-CNF, el recubrimiento era perjudicial para la colonización bacteriana. Teniendo en cuenta el efecto del T-CNF observado en las bacterias, desarrollamos un recubrimiento de T-CNF/alcohol polivinílico (PVA) reticulado químicamente con un excelente rendimiento antibioincrustante, eficiente adsorción/rechazo de iones, además de exclusión por tamaño y con estabilidad dimensional y de pH. Más adelante, utilizamos un enfoque de impregnación de superficies basado en nanotecnología con base biológica que dio como resultado membranas de filtración de agua altamente eficientes, para flujos voluminosos, y con propiedades mecánicas mejoradas. Además, este fue un enfoque totalmente renovable basado en textiles no tejidos disponibles comercialmente. Las membranas con recubrimientos preparados a partir de CNC, nanocristales de quitina (ChNC) y T-CNF separaron partículas en el rango de tamaño de bacterias y virus. Adicionalmente, las preparadas a partir de T-CNF mostraron una alta eficiencia de filtración de microplásticos. En el caso del revestimiento de membrana basado en ChNC y T-CNF tenía excelentes propiedades antibacterianas.

En general, demostramos la capacidad multifuncional de nuestros recubrimientos; incluyendo una reducción significativa de las incrustaciones orgánicas, la mejora en adsorción de iones, separación de microplásticos y reducción efectiva de la formación de biopelículas. En el caso de este último, el grupo funcional, la carga superficial y la hidrofiliidad de los diferentes nanopolisacáridos determinaron el efecto sobre las bacterias, mostrando un excelente potencial para adaptar superficies contra microbios. Además, hicimos un estudio comparativo directo para definir el efecto entre los diferentes nanopolisacáridos de interés (CNC, T-CNF, L-CNC y ChNC) sobre la viabilidad bacteriana y la formación de biopelículas, mostrando una gran diferencia en el efecto citostático impartido por los diferentes tipos de nanocelulosa y nanoquitina. En paralelo, las propiedades nanomecánicas de las células bacterianas y las fuerzas entre los nanopolisacáridos y *Escherichia coli* (*E. coli*) se vieron afectados al estar en contacto directo con las superficies de T-CNF, L-CNC y ChNC.

Por último, fuimos capaces de trasladar con éxito uno de nuestros procesos de recubrimiento a una planta piloto, demostrando que el método podría implementarse fácilmente a nivel industrial. El impacto de esta tesis se basa en la efectividad de los recubrimientos, los diferentes tipos de funcionalidades observadas, la rápida implementación demostrada a escala industrial y el potencial para extrapolar esta tecnología a otras aplicaciones.

List of publications

This thesis is written based on the following publications:

I. Waterborne nanocellulose coatings for improving the antifouling and antibacterial properties of polyethersulfone membranes

Andrea Aguilar-Sánchez, Blanca Jalvo, Andreas Mautner, Samer Nameer, Tiina Pöhler, Tekla Tammelin and Aji P. Mathew. Journal of Membrane Science (2021) 620, 118842.

My contribution: conceptualization, investigation, methodology, validation and writing the original manuscript.

II. Charged ultrafiltration membranes based on TEMPO-oxidized cellulose nanofibrils/poly(vinyl alcohol) antifouling coating

Andrea Aguilar-Sánchez, Blanca Jalvo, Andreas Mautner, Ville Rissanen, Katri S. Konturi, Hani Nasser Abdelhamid, Tekla Tammelin and Aji P. Mathew. RSC Advances (2021) 11, 6859-6868.

My contribution: conceptualization, investigation, methodology, validation and writing the original manuscript.

III. Water Filtration Membranes Based on Non-Woven Cellulose Fabrics: Effect of Nanopolysaccharide Coatings on Selective Particle Rejection, Antifouling, and Antibacterial Properties

Blanca Jalvo, Andrea Aguilar-Sánchez, Maria-Ximena Ruíz-Caldas and Aji P. Mathew. Nanomaterials (2021) 11(7), 1752.

My contribution: investigation, methodology, validation and editing the manuscript.

IV. Revealing the interaction between nanopolysaccharides and *E. coli* by biological studies and atomic force microscopy

Andrea Aguilar-Sánchez[†], Jing Li[†], Andreas Mautner, Blanca Jalvo, Edouard Pesquet and Aji P. Mathew. Manuscript in progress (2022)

[†]Indicates shared first authorship.

My contribution: conceptualization, investigation, methodology, validation and writing the original manuscript.

V. Pilot-scale modification of polyethersulfone membrane with a size and charge selective nanocellulose layer

Tiina Pöhler[†], Andreas Mautner[†], Andrea Aguilar-Sánchez[†], Björn Hansmann, Vesa Kunnari, Antti Grönroos, Ville Rissanen, Gilberto Siqueira, Aji P. Mathew and Tekla Tammelin. Separation and Purification Technology (2021) 285, 120341.

[†]Indicates shared first authorship.

My contribution: investigation, methodology, validation, writing and editing the original manuscript.

Publications not included in this thesis:

VI. Bio-based Micro-/Meso-/Macroporous Hybrid Foams with Ultrahigh Zeolite Loadings for Selective Capture of Carbon Dioxide

Luis Valencia, Walter Rosas, Andrea Aguilar-Sánchez, Aji P. Mathew and Anders E. C. Palmqvist. ACS Applied Materials and Interfaces (2019) 11, 40424–40431.

My contribution: investigation, methodology, validation and editing the original manuscript.

VII. 3D-printable biopolymer-based materials for water treatment: A review

Natalia Fijol, Andrea Aguilar-Sánchez and Aji P. Mathew. Chemical Engineering Journal (2022) 430, 132964.

My contribution: conceptualization, investigation, and editing the original manuscript.

VIII. Bio-elastomers: current state of development

Ilse Magaña, Ricardo López, Francisco Javier Enríquez-Medrano, Sugam Kumar, Andrea Aguilar-Sánchez., Rishab Handa, Ramón Díaz de León and Luis Valencia. Journal of Materials Chemistry A (2022) 10, 5019-5043.

My contribution: investigation, and editing the original manuscript.

IX. 3D-printed PLA biocomposite filters reinforced with TEMPO-oxidized cellulose nanofibers and chitin nanocrystals for water treatment.

Natalia Fijol, Andrea Aguilar-Sánchez, Stephen Hall, Aji P. Mathew. Manuscript in progress (2022)

My contribution: investigation, methodology, validation and writing the original manuscript.

Book chapter:

X. Nano Hydrogels: Physico-chemical properties and recent advances in structural designing

Luis Valencia, Andrea Aguilar-Sánchez, Francisco Javier Enriquez-Medrano, Ramón Díaz de León. Nano hydrogels: Physico-chemical properties and recent advances in structural designing, ed. J. Jose, S. Thomas and V. K. Thakur, Springer Singapore, Singapore, 2021, pp.135-150.

My contribution: investigation and writing.

Conferences

Conferences attended during the studies:

I. Engineering with membranes Conference 2019, Båstad, Sweden.

Andrea Aguilar-Sánchez, Blanca Jalvo, and Aji P. Mathew.

Poster presentation: Nano-cellulose coatings for antifouling polyethersulfone (PES) membranes.

II. Nordic Polymer Days 2019, Trondheim, Norway.

Andrea Aguilar-Sánchez, Blanca Jalvo, and Aji P. Mathew.

Poster presentation: Nano-cellulose coatings for antifouling and mechanically enhanced polyethersulfone (PES) membranes.

III. Annual Surface and Materials Chemistry Symposium 2021, Stockholm, Sweden.

Andrea Aguilar-Sánchez, and Aji P. Mathew.

Oral presentation: Waterborne functional coatings based on polysaccharide nanoparticles.

IV. American Chemistry Society 2022, San Diego, CA, USA.

Andrea Aguilar-Sánchez, and Aji P. Mathew.

Oral presentation: Nanocellulose coatings as a multifunctional surface modifier.

Contents

1.	Introduction.....	3
1.1	Membrane technology.....	4
1.1.1	Separation mechanisms.....	5
1.1.2	Common filtration systems: polymeric membranes and non-woven fabrics	6
1.1.3	Common problems in membrane performance.....	7
1.2	Nanopolysaccharides	10
1.2.1	Nanocellulose.....	11
1.2.2	Nanochitin.....	14
1.3	Scope of the thesis	15
2.	Methodology	17
2.1	Preparation of materials	17
2.2	Surface modification/coating techniques	19
2.3	Characterization methods.....	21
3.	Functionalized nanopolysaccharide coatings to enhance commercially available membranes and non-woven fabrics	31
4.	Revealing the effect of nanopolysaccharide-based coatings on bacterial viability	39
5.	From lab-scale to pilot line: Scalability of coatings for commercialized PES membranes	45
6.	Summary and future work	51
7.	Acknowledgements.....	53
8.	References.....	55

Abbreviations

AFM	Atomic force microscopy
BET	Brunauer–Emmett–Teller
BJH	Barrett-Joyner-Halenda
BSA	Bovine serum albumin
CFU	Colony forming unit
ChNC	Chitin nanocrystals
CNC	Cellulose nanocrystals
DI	De-Ionized
DLS	Dynamic Light Scattering
<i>E. coli</i>	<i>Escherichia coli</i>
FT-IR	Fourier transform infrared microscopy
GA	Glutaraldehyde
IUPAC	International Union of Pure and Applied Chemistry
LB	Lysogeny broth
L-CNC	Ligno-cellulose nanocrystals
MF	Microfiltration
MO	Methyl Orange
MWCO	Molecular weight cut-off
NB	Nutrient broth
NF	Nanofiltration
OD ₆₀₀	Optical density measured at wavelength 600 nm
OFR	Organic fouling resistance
PAHCl	Poly(allylamine) hydrochloride

PBS	Phosphate-buffered saline
PES	Polyethersulfone
PSS	Polystyrene sulfonates
PVA	Poly(vinyl alcohol)
PVDF	Polyvinylidene fluoride
QCM-D	Quartz crystal microbalance and dissipation
RH	Relative humidity
RO	Reverse osmosis
SDS	Sodium dodecyl sulfate
SEM	Scanning electron microscopy
T-CNF	TEMPO-oxidized cellulose nanofibrils
UF	Ultrafiltration
UV-vis	Ultraviolet visible spectrophotometry
VB	Victoria Blue
XPS	X-Ray photoelectron spectroscopy

1. Introduction

Water scarcity affects more than 40% of people worldwide and this number is expected to rise due to climate change¹. The increase of drought and desertification on all the continents will result in at least one-fourth of the population suffering from recurring water shortages by 2050¹. In addition, water sources are being constantly polluted with land-based sources, rapidly escalating the water scarcity problem. For example, it is estimated that there is an average of 13 000 pieces of plastic litter per square kilometer in the ocean¹. Furthermore, achieving sustainable development will require that we reduce our ecological footprint by changing the way resources are produced and consumed¹. The United Nations Global Goals for Sustainable Development encourage countries to invest in sustainable solutions and minimize fossil-fuel subsidies¹. This leaves material chemists, among others in the scientific community, the great responsibility of substituting current petroleum-derived products with renewable options of equal performance as their commercial counterparts.

This thesis navigates through several challenges related to water-treatment membranes used in different industrial processes. It focuses on improving the performance of available commercial products to reduce waste and energy consumption, while dealing with the substitution of the current petroleum-derived products to options derived from renewable sources.

Surface functionalization is a straightforward option for improving the currently available membranes and fabrics in the market. Most specifically, coatings are a type of surface modification approach, that do not interfere with the bulk properties of the pristine materials, and that functionalizes surfaces without needing great amounts of the new material. Materials in the nanometric scale, i.e. one or more dimensions shorter than 100 nm, such as nanocellulose and chitin nanocrystals, are promising options for different types of surface functionalization, including antifouling, antimicrobial, contaminant adsorption, and mechanical enhancement, along with others²⁻¹⁸.

1.1 Membrane technology

Membranes are barriers that work by selectively allowing some species to pass while others are stopped². They are heavily used in separation processes, including water and wastewater treatment. They efficiently and reliably remove contaminants without adding new chemicals or generating harmful byproducts in water-treatment processes. The selectivity and removal efficiency of a membrane depend on its microstructural characteristics, pore size, and surface chemistry. Pore size and surface chemistry can be controlled during the manufacturing process or subsequent steps².

Spontaneously, species move from regions of high concentration to low concentration. Pressure-driven membrane filtrations, including microfiltration (MF), ultrafiltration (UF), nanofiltration (NF) and reverse osmosis (RO), use pressure gradients to cause contaminants to flow from regions of low to high concentration and thus purify the water¹⁹. Membranes with smaller pore sizes must be operated under higher pressure¹⁹ (see Figure 1.1).

Membranes with pores bigger than 1 nm are defined as porous membranes, including MF and UF membranes¹⁹, which are the main focus of our work. They predominantly separate species via size exclusion (see section 1.1.1). MF membranes are extensively used in the primary disinfection of uptake wastewater streams, where they present a physical means of separation, having a barrier-like effect. They allow both filtration and disinfection to take place in a single step, avoiding the use of chemical separation methods. UF membranes are the most commonly used in water treatment, the pharmaceutical industry, food, and beverage production. They separate particles and macromolecules in the range of 1 to 100 nm from a fluid feed and they are classified by their nominal molecular weight cut-off (MWCO), which is the molecular weight of a solute rejected 90%.

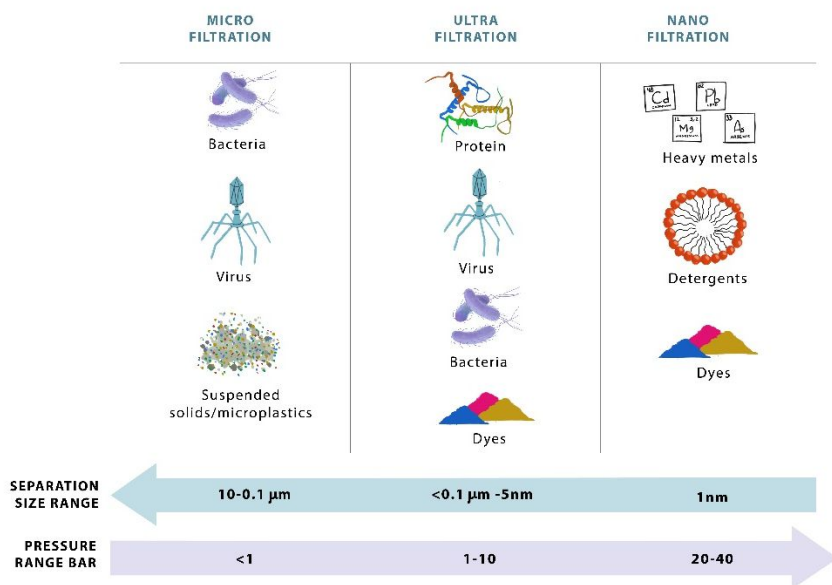


Figure 1.1 Schematic representation of separation size and pressure range for the pressure-driven membranes of interest.

1.1.1 Separation mechanisms

The main mechanism of separation across pressure-driven filtration is size exclusion; nevertheless, mechanisms including adsorption, absorption, flocculation, and coagulation, have also been adopted in separation processes, and most specifically for water purification treatment¹⁹. The studies developed during this thesis were focused on size exclusion and adsorption (see Figure 1.2).

In separation by size exclusion, everything larger than the pore size is rejected, while smaller species flow through the membrane. This is the main mechanism present in MF and UF membranes, whose pore sizes define the contaminants that they can filter. The International Union of Pure and Applied Chemistry (IUPAC) divides membranes into categories based upon their pore sizes: nano (0.1–100 nm), micro (0.1–100 μm), and milli (0.1–100 mm). Membranes can remove multivalent ions, viruses, bacteria, and suspended

particles depending on the membrane or filter used²⁰. Furthermore, the pressure required for a successful separation process is higher as the pore size decreases.

Among the multiple treatment methods available for ion removal, adsorption is the most cost-efficient and simple²¹. In this process, cationic or anionic groups attached to the surface of an electrically charged membrane repel like-charged species, preventing them from attaching to the surface, or conversely, enable the tailored adsorption of opposite-charged species²². This can be accomplished using nanoscaled materials, due to their high specific surface area. Functional groups on the nanoparticle surfaces can interact with different chemical groups, molecules, atoms, or ions in the media and enhance the selective removal of some chemical species²³.

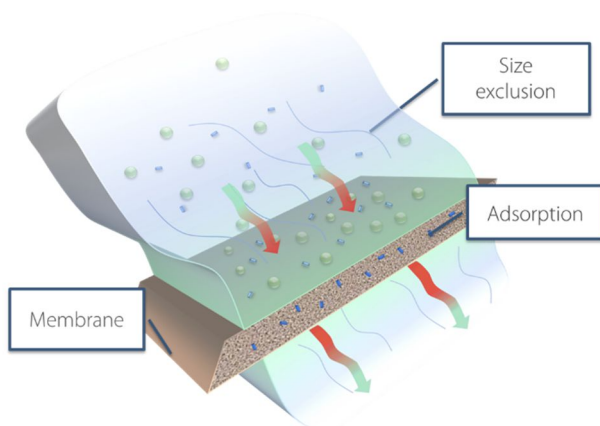


Figure 1.2 Schematic representation of the membrane's separation mechanisms of interest.

1.1.2 Common filtration systems: polymeric membranes and non-woven fabrics

The four major filtration systems on the market are membranes, non-woven and woven fabrics, and paper; all of these are engineered to meet the exact specifications and requirements for air and liquid filtration. Our studies focused on the modification of polymeric membranes and non-woven fabrics due to their extensive usage in the industry.

Polymeric membranes are widely used for separation purposes in feed streams that contain ions, molecules, and colloids²⁴. The most common separation ranges for this type of membranes are the microfiltration (MF) regime, which covers several micrometer-sized particles; and the ultrafiltration (UF) regime, with the second-largest pore size, as mentioned in the previous section. Although polymeric membranes are commonly used in filtration, only a few polymer types have the required chemical resistance, thermal stability, good mechanical properties, and ease of processing²⁴. Some of the most common polymers used for filtration are polysulfone (PSf), poly(ether sulfone) (PES), poly(vinylidene fluoride) (PVDF), cellulose acetate (CA), polypropylene (PP), poly(acrylonitrile) (PAN) and polyamides (PA)²⁴. Polyethersulfone (PES) is the prevailing polymer used for porous MF and UF membranes. Its structure consists of repeating units of ether and sulfone linkages alternating between benzene rings. PES is thermally stable, tough, and resistant to mineral acids. However, as PES is hydrophobic, it must be modified to upgrade its performance as a membrane for water filtration³.

The second most common option is non-woven fabrics. They offer unique technical characteristics, such as great permeability, large specific surface area, and controllable pore size distribution. The filtration mechanisms relevant to non-woven fabrics provide good filtration efficiency, low energy consumption, and great foulant-cake discharge properties²⁵ and therefore, longer service life. The structures of non-wovens can be tailored via different manufacturing methods and materials for use in diverse applications. When compared to membranes, wire cloth, or monofilament fabrics; non-woven fabrics offer a thicker cross-section and bulk, which provides them with the features necessary to fulfill the requirements and boundary conditions of all types of applications²⁶.

1.1.3 Common problems in membrane performance

Fouling

One of the main problems that membranes face during usage is fouling, which is the deposition of undesired material on a surface or within the pores, and leads to some type of malfunction. The problems that can arise from a fouled surface include loss of production efficiency, product spoilage, and safety issues, among others. In water- and wastewater-treatment systems, fouling can

cause corrosion and decrease the quality of treated water, as well as reduce the permeation flux, which in turn increases the energy demand and operational and maintenance costs^{24,27–30}. Overall, fouling lowers the efficiency of the membrane, but it can be mitigated by modification of the membrane's surface.

Most of the foulants are complex, and how prone a membrane is to fouling depends on the attractive forces between the membrane and the foulants²⁴. Foulants can be organic, inorganic, or living organisms. The most common foulants in water purification membranes are proteins or macromolecules, emulsified oil, microorganisms (also known as “biofouling”), natural organic matter, and minerals²⁴. We focused mostly on proteins and biofouling; therefore, we will refer to proteins and macromolecules as organic foulants, and to bacteria as biofouling.

Organic foulants, such as proteins, are denatured upon contact with a surface, which promotes further protein deposition³¹. The interaction between the proteins and a surface is a combination of hydrophobic, electrostatic, and hydrogen bonding forces³¹. Protein deposition can be strongly reduced on hydrophilic surfaces, compared to hydrophobic surfaces³².

Biofouling is the term used for the accumulation of microorganisms, plants, algae, or animals. The biggest difference between organic fouling and biofouling is that the latter is characterized by cell proliferation and formation of a biofilm, while this is not the case for organic fouling. Biofilms are microbial communities embedded in a matrix of extracellular polymeric substances, which facilitates their survival in adverse environments. Microorganisms adhere to surfaces through interactions such as van der Waals, electrostatic, hydrogen bonding, and hydrophobic interactions^{33,34}. Extracellular polymeric substances, which containing polysaccharides and proteins, are secreted by the microorganisms and reinforce the biofilm^{34,35}. Biofilm formation differs between the bacterial strains, but the general phases of its development are (1) initial adhesion to the surface (reversible), (2) irreversible coupling or growth division, (3) formation of microcolonies, (4) development of the microcolonies and biofilm formation, and (5) once the biofilm is developed, some of the bacteria are released to colonize new environments^{29,30,36}. Since bacterial adhesion is one of the initial phases of biofilm formation, it can be prevented or reduced by tailoring the properties of the surface in which the microorganisms might be in contact, thus reducing fouling.

Factors that influence fouling

To understand surface fouling, it is necessary to consider factors such as surface charge, hydrophilicity, roughness and topography (see Figure 1.3), and in the case of biofouling, it is also necessary to consider the interactions of the bacterial appendages with the surface. The best approach to improve the antifouling properties of a surface is to tailor it in a way that takes into account the previously mentioned factors; like for example by adding functional hydrophilic or charged nanomaterials, or by smoothening the surface by surface treatment^{2,3,11,12,24,37}. We will go into more details on the influence of each factor in the further paragraphs; nevertheless, it is important to emphasize that, even when the surface is tailored, environmental factors, such as temperature or pH, within others, can influence fouling.

The binding interaction between a foulant and a surface can be altered by tailoring the surface charge of the latter²⁷. This means that, if most bacterial cells or organic foulants are negatively charged, a good strategy to repel them is by preparing a negatively charged surface; while a positively charged surface will be more prone to fouling. However, it is known that some cationic groups, such as quaternary ammonium ions and polyethylenimines, attract microorganisms by electrostatic interactions and might kill them due to their antimicrobial activity³⁸.

Surface energy can be altered by tuning the hydrophobicity of a surface. This will depend on the type of foulant that is to be avoided. Improving the hydrophilicity of a surface can allow it to bind water molecules (also known as surface hydration), avoiding the adherence of possible foulants³⁹. In the specific case of biofouling, both superhydrophilic and superhydrophobic surfaces can provide a non-fouling effect²⁷.

Another way to reduce fouling and biofilm formation can be accomplished by smoothening the surface. Rougher surfaces have a greater contact area between foulants and the surface, and also shield foulants from shearing forces²⁷. Once again, the effect of this factor will depend on the size and type of foulant and are distinctive of the surface material composition²⁷.

In the specific case of biofoulants, both the topography and stiffness of a surface influence biofilm formation²⁷. Some topographic patterns, such as nanopillars, can affect bacterial proliferation⁴⁰. Likewise, material stiffness affects bacterial adhesion, although, the mechanism of the effect is not defined yet²⁷.

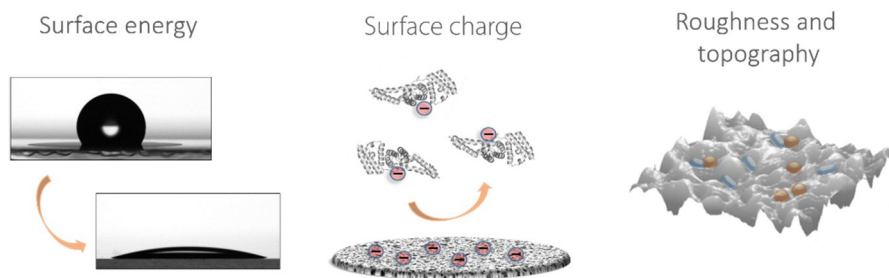


Figure 1.3 Schematic representation of the factors that influence fouling. Surface energy image taken from platypustech webpage and adapted with their permission.⁴¹

1.2 Nanopolysaccharides

Polysaccharides are formed by multiple saccharide units linked together by glycosidic linkages, extracted from plants, microbes or animals. They have stereoregular chemical structure of repeating units of glucose, and their general chemical formula is $(C_6H_{10}O_5)_n$. Properties such as three-dimensional arrangement, molecular size, and physicochemical properties, depend on the type of substituents attached to the intercalated chains of the polymers, linkage pattern, number, and location of the branching monomers within the polymer chains⁴².

In this thesis, we focus on nanopolysaccharides that can be obtained from plants or shellfish shells by chemical and mechanical treatments, then dispersed in aqueous or organic solvents. The process for obtaining polysaccharide nanofibers/nanocrystals does not break them down to the molecular level of the polysaccharide chains, but only breaks down the structure to a nanoscale fiber with very high degree of crystallinity. This assures the retention of and enhances the most desired material properties, such as high tensile strength, high chemical resistance, along with others. The surface of a nanopolysaccharide can be chemically modified to add a specific functionality¹².

Cellulose nanocrystals (CNC), ligno-cellulose nanocrystals (L-CNC), cellulose nanofibrils (CNF), TEMPO-oxidized cellulose nanofibrils (T-CNF), and chitin nanocrystals (ChNC), possess high surface activity, surface charge, and surface area required to tailor specific features such as nanostructured and

nano-enabled bio-based membranes. These nanomaterials also have good film-formation ability²⁶, which is a highly required feature in coating and surface-treatment applications. Furthermore, they provide a nanoscaled architecture on the substrate where they are applied, which positively contributes to the final material performance and modified properties such as mechanical strength, durability, stability, wettability, along with others. In addition, they have shown certain antifouling activity^{13,43}. Previous studies have revealed the outstanding performance of nanocellulose and nanochitin as functional materials for novel water purification membranes^{2,13–16}.

1.2.1 Nanocellulose

Cellulose is the most abundant polymer on Earth, and the dominant component of plants (Figure 1.4), bacteria, algae, fungi, and certain animals such as tunicates. Cellulose fibrils can be extracted from a broad variety of biomass, providing the possibility of an inexpensive, abundant, and sustainable option¹⁹. In plant cell walls, nanocellulose is synthesized in as nanosized fibrils that consist of aligned molecular chains of high crystallinity, therefore it is renewable, abundant and biodegradable. In recent years, it has been increasingly exploited as a versatile bio-based option for membrane applications. Its nanoscale morphology, surface chemistry, the ability to produce charged nanometric layers, high specific surface area and large number of active sites for the interaction with charged entities^{12,17,44,45}, among others, are the higher valued properties which make nanocellulose ideal for separation technology. The mechanisms in which nanocellulose membranes facilitate rejection are (i) adsorption, due to charged surfaces; (ii) size exclusion from the nanoscaled porous networks formed; (iii) a combination of both^{2,18}. These are basically the same principles by which conventional charged membranes work.

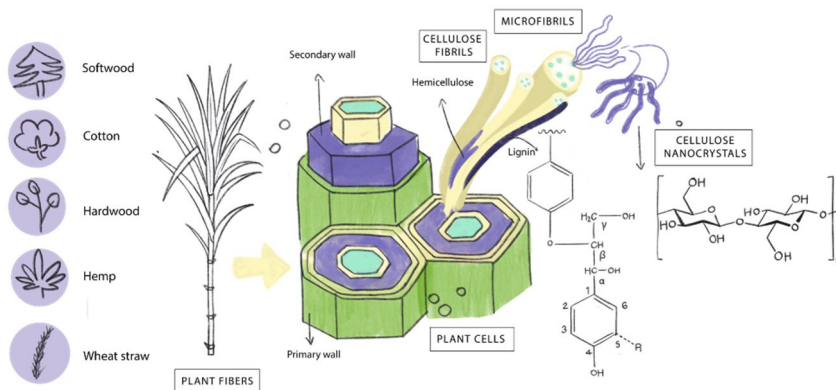


Figure 1.4 Schematic representation of the hierarchical structure of cellulose.

Ligno-cellulose nanocrystals (L-CNC)

The term "lignocellulosic materials" is used to describe plants that are composed of cellulose, hemicellulose, and lignin⁴⁶. As shown in Figure 1.4, lignin is present in plant cell walls, embedded with cellulose and hemicellulose, and it is the main aromatic polymer in Nature. It consists of amorphous 3D branched aromatic molecules that contain methoxyl groups, aliphatic and phenolic hydroxyl groups, and carboxylic acid groups in the side chains (Figure 1.5 a)⁵⁰. This complex structure provides lignin with a range of properties such as high carbon content, high thermal stability biodegradability, antioxidant activity, and antimicrobial properties, among others⁵⁰.

Cellulose nanocrystals (CNC)

Cellulose nanocrystals (CNC) are isolated by acid hydrolysis to remove pectin, hemicelluloses, and lignin. The "disordered" or para-crystalline regions of cellulose are hydrolyzed in this process; while the crystalline regions remain intact due to their higher resistance to acid hydrolysis⁴⁷. The final product has a rod-like shape⁴⁷, with an anionic charge on the surface due to acid hydrolyzation⁴⁸. The CNCs used in our studies have negative sulfate half-ester groups on the surface of the crystals from the hydrolysis with sulfuric acid (Figure 1.5 b)⁴⁷.

The addition of CNC to polymeric composites is used to modify different characteristics of the material¹¹. In general, CNC improves the hydrophilicity of the materials due to the abundant hydroxyl groups in its structure³. Due to the high hydrophilicity of CNC, it shows a great capability to be dispersed in water, polar solvents, and water-soluble polymers¹¹.

TEMPO-oxidized cellulose nanofibrils (T-CNF)

Cellulose nanofibrils can be individualized by surface carboxylation using (2,2,6,6-tetramethylpiperidin-1-yl)oxyl (TEMPO) to catalyze partial oxidation of the primary hydroxyl and carboxyl groups of the polysaccharides with sodium hypochlorite in the presence of a small amount of sodium bromide⁴⁸ at ambient temperature. This yields carboxyl and aldehyde groups. Polysaccharide fibers are broken up and loose bundles of nanofibers are obtained. Additional mechanical disintegration can be performed.

The partially carboxylated surface of TEMPO-oxidized cellulose nanofibrils are decorated with hydroxyl and carboxyl groups (Figure 1.5 c), making them intrinsically hydrophilic and negatively charged at a pH range different to low acidic conditions¹². The high specific surface area, i.e. surface-to-volume ratio, as well as high surface charge density are some of the advantageous characteristics they have that are useful for reducing biofouling and organic fouling^{4,5,49} in water purification and separation technologies^{2,12}.

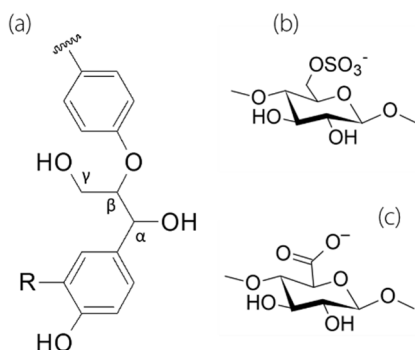


Figure 1.5 Chemical structures of interest: a) lignin, b) CNC, and c) T-CNF.

1.2.2 Nanochitin

Chitin is a biologically abundant polymer that can be found in 70% of all living organisms⁵¹ (see Figure 1.6), being the second most common polysaccharide in Nature, after cellulose²⁶. Its main commercial source is the crustacean wastes of the fishing industry since it is the main organic component of the skeletal structure of arthropods, mollusks, and annelids²⁶. The difference between chitin and cellulose structure consists of the group present at carbon C2, which in cellulose is a hydroxyl group, while in chitin is an acetamide group²⁶. Chitin is a linear polysaccharide that consists of $\beta(1\rightarrow4)$ linked units of *N*-acetyl-2-amino-2-deoxy-D-glucose. Depending on the source, a proportion of the structural units are deacetylated in natural chitin²⁶. Chitin isolation processes start by conditioning the raw material, continue via deproteinization or protein extraction, the removal of inorganic components or demineralization, and lastly decolorization²⁶; although the order of the steps depends on the final usage and requirements for the chitin.

Some of the most important characteristics of chitin are nontoxicity, biodegradability, edibility, biocompatibility, antioxidant, antimicrobial, and thermally stability, providing it with a wide range of fields in which it can be employed⁵¹.

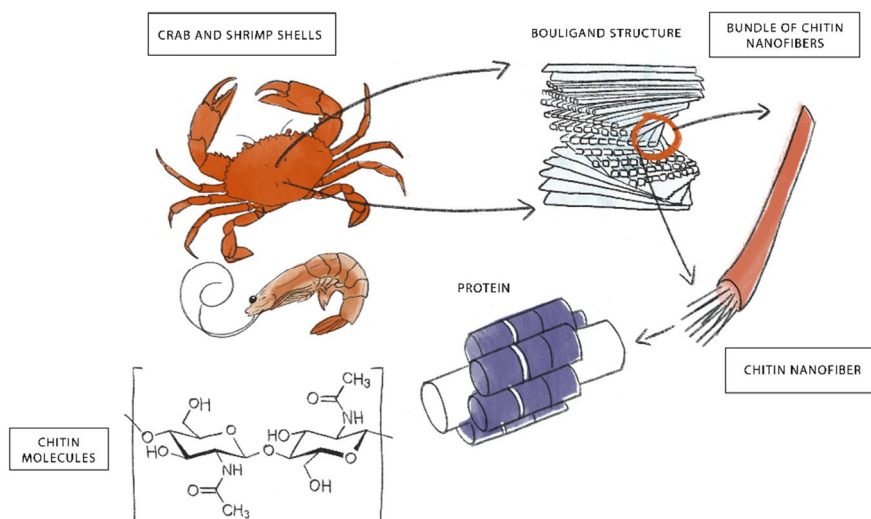


Figure 1.6 Schematic representation of the hierarchical structure of chitin.

1.3 Scope of the thesis

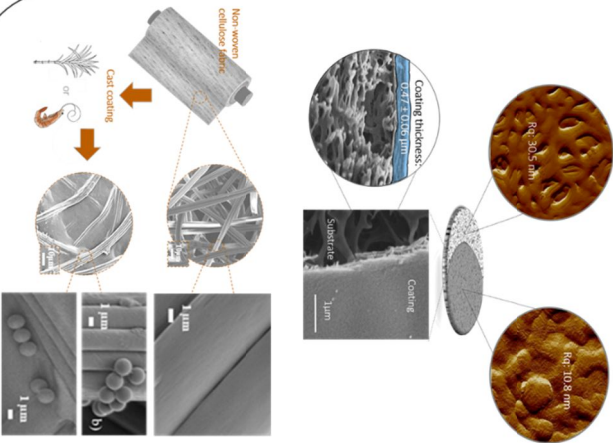
The main goal of this thesis was to develop scalable bio-based coatings for functional membranes. Most specifically, this work was centered on modifying the surface of commercially available polyethersulfone (PES) and non-woven cellulose fabrics, using different types of nanopolysaccharides. This included using cellulose nanofibers/crystals and chitin nanocrystals to provide to the membranes with specific functionality and to yield more efficient, longer usage-life, cost-effective and environmentally friendly products, and with new functionalities, compared with the currently available ones. In addition to developing an adequate method for the surface modification, we characterized the membranes to show the tailored functionalization and how the current product was further improved. The functions targeted for development were antibiofouling, increase in hydrophilicity, pH resistance, superior wet strength, size exclusion, and charge-specific surface adsorption/rejection.

The second objective was to compare the different effects that nanopolysaccharides have on bacterial proliferation, both when in direct contact with bacteria or within media prone to bacterial proliferation. This is considered one of the most interesting features and potential fields in which materials from renewable resources can be used.

The final objective was to develop a deeper understanding of the effect of material variables and the process parameters to transfer laboratory results to scalable processes. Therefore, the most favorable results obtained in the laboratory were transferred to the SUTCO pilot line at VTT Technical Research Centre of Finland. Figure 1.7 presents the different goals targeted along the thesis.

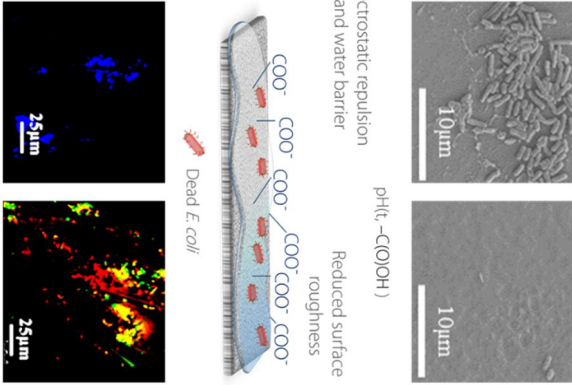
Functionalized nanopolysaccharide coatings to enhance commercially available membranes and non-woven fabrics

Paper I, II, III



Revealing the effect of nanopolysaccharide-based coatings on bacterial viability

Paper I, II, III, IV



From lab-scale to pilot line: Scalability of coatings for commercialized PES membranes

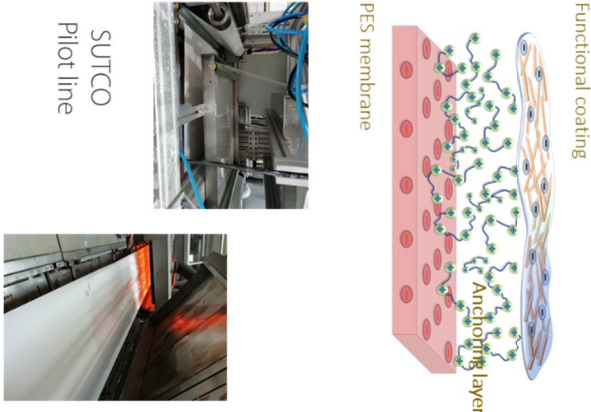


Figure 1.7 Schematic representation of the subtopics studied along this thesis.

2. Methodology

2.1 Preparation of materials

Throughout our work, we used five types of functional nanoparticles: (i) CNC, (ii) T-CNF, (iii) L-CNC, (iv) CNF, and (v) ChNC. CNC was purchased from Celluforce, Canada and was obtained by the well-established sulfuric acid hydrolysis⁴⁷. For *paper I-IV*, T-CNF was provided by Swiss Federal Laboratories for Materials Science and Technology (EMPA), Switzerland. For *paper V*, it was prepared at VTT Technical Research Centre of Finland, Finland. The T-CNF used was prepared following the procedure reported by Isogai et al.⁵². The next paragraphs explain the procedure followed in our lab to obtain L-CNC, CNF, and ChNC; as well as the procedure followed to produce nanopolysaccharide films as well as their sterilization method used in *paper IV*.

Lignocellulose nanocrystals (L-CNC)

For *paper IV*, the L-CNC was obtained following the procedure reported by Georgouvelas et al.⁶ Residues from the production of bioethanol were partially bleached. 30 g of pulverized extractive-free residue was combined with 10 g of NaClO₂ and 4 mL of CH₃COOH in 2 L of H₂O. The reaction mixture was stirred for 1 h at 70 °C, and then another 10 g of NaClO₂ and 4 mL of CH₃COOH were added. Afterwards, the material was washed with H₂O via centrifugation, the material was suspended in water at ~1% (w/w) and sonicated with a titanium rod sonifier (QSonica sonicators, Q500) at 24 kHz for 10 min to avoid the presence of large aggregates. The resulting dispersion was then passed 10 times through an APV 2000 high-pressure homogenizer at a pressure of 600–800 bar. After homogenization, the obtained nanocrystals were dialyzed against Milli-Q water by using a 14000 Da molecular weight cut-off dialysis membrane (Sigma-Aldrich) for one day. The amount of residual lignin in the lignocellulosic material was quantified to 6.0 ± 0.4% (w/w), with the use of the TAPPI method T222, also known as the Klason method, considering both the acid-soluble and -insoluble parts of lignin⁶.

Cellulose nanofibrils (CNF)

For *paper V*, the CNF was obtained from dried bleached birch kraft pulp from a Finnish pulp mill (Metsä Fibre, Finland). It was mechanically disintegrated without chemical modification. The pulp, with a carbohydrate content of 73 wt% glucose, 23 wt% xylose and 0.15 wt% methyl glucuronic acid, was first soaked in deionised water (1.8 w% pulp) overnight and dispersed using a high-shear Ystral X50/10 Dispermix mixer (Ystral, Germany) for 20 min at 1770 rpm. The pulp suspension was passed twice through a Masuko grinder (Supermasscolloider MKZA10-15 J, Masuko Sangyo Co., Japan) at 1500 rpm and then fluidised (Microfluidics M-7125-30, Microfluidics Corp., USA). The suspension was run through the 400 µm chamber at 50 bar, then fibrillated at 1800 bar via one pass through the chambers with diameter of 400 µm and 200 µm, and then five passes through the 400 µm and 100 µm chambers⁵³

Chitin nanocrystals (ChNC)

For *paper III* and *IV*, the ChNC were obtained following the procedure explained by Jalvo et al.⁵⁴ Deproteinized and bleached shrimp chitin flakes were hydrolyzed in 3 N hydrochloric acid at 90 °C for 90 min. The resulting suspension was centrifuged to remove the excess acid and the less-dense acid fraction was decanted away to leave a turbid suspension of chitin nanocrystals. This chitin nanocrystal suspension was dialyzed against distilled water to achieve a pH of 5.6 in the suspension, and finally homogenized and sonicated to ensure separation of the individual nanocrystals prior to storage⁵⁴.

Nanopolysaccharides film preparation

The samples were prepared by pressurized filtration. A 10–15 mL portion of the nanopolysaccharide suspension was filtered through polyvinylidene fluoride (PVDF) membrane, having a pore size of 0.45 µm, using a vacuum gas pump until all the water was removed and a dry film was formed. The final film produced was a circular film with a diameter of 47 mm.

Film sterilization method

For *paper IV*, inside a laminar flow hood, each film was placed inside an autoclaved Erlenmeyer flask using a sterile tweezer. A prepared solution of 70 v% EtOH in with sterile Milli Q water was added, covering the entire film for 10 min. Later, the EtOH was removed and the film was washed twice, each

time for 5 min, using sterile Milli Q water. Subsequently, the sterile Milli Q water was removed and the film was soaked in aqueous 0.1% calcium hypochlorite/0.0001% Triton x100 solution for 20 min, covering the entire film. The solution was removed and once again, the film was washed twice with sterile Milli Q water for 5 min each time, and then once with 70 v% EtOH for 10 min, and two last sterile Milli Q water washes were done for 5 min each. Lastly, the sterile Milli Q water was removed and lysogeny broth (LB) medium was added, covering the film completely. Cotton and aluminum foil were added to the top of the flask, which was removed from the laminar flow hood and incubated at 37 °C with agitation overnight.

2.2 Surface modification/coating techniques

Layer-by-layer coating technique on PES membranes

For *papers I* and *V*, the surfaces of the membranes were modified using layer-by-layer deposition.

Paper I uses a laboratory-scale approach in which the PES membranes were immersed for 1 min in a 0.6 wt% aqueous solution of PAHCl, then rinsed thrice using deionized water. Subsequently, nano-cellulose suspensions (1 wt% CNC or T-CNF) were cast coated at a speed of 1 mm s⁻¹, with a gap distance of 100 µm, using an automatic film applicator (Elcometer 4340 motorised). Afterwards, the coated membranes were dried for 20 min at 100 °C.

Paper V exposes a pilot-scale coating procedure by cast-coating and spray-coating techniques. A blend of 75 wt%-25 wt% CNF-T-CNF was mixed using a high-speed disperser (Diaf Pilvad, Denmark) at 700 rpm. Next, the nanocellulose blend suspension was diluted to a concentration of 0.6 wt% and the pH was adjusted to 4 with 0.1 M HCl. The PES membrane film was plasma-treated (Ar-plasma, 2000 W m⁻² h⁻¹, Vetaphone, Denmark) to activate and clean the membrane surface. A 0.1 wt% b-PEI solution was applied by guiding the membrane through a basin filled with the polymer solution. The residence time of the membrane in the b-PEI bath was approximately 10 s. Then the membrane was subsequently led to a washing basin filled with deionised water resulting in approximately 60 s. Two different coating methods, either cast coating or spray coating were employed to apply 0.6 wt% nanocellulose dispersions on PES membranes with the target dry layer

thickness below 1 μm . The cast coating was performed by feeding nanocellulose manually to the open casting slot equipped with a doctor blade. The level of nanocellulose dispersion in the slot was kept constant to prevent variations of the coat weight and thus masses of the dispersion caused by the effect of gravity. The metering gap was 100 μm , equal to the wet coating thickness. Spray coating was performed by using a Graco 512 nozzle with 305 μm orifice, with 0.15 MPa pump pressure and 0.4 MPa nozzle pressure. The speeds during coating were 1 or 5 m min^{-1} , for cast coating, and 5 or 7 m min^{-1} , for spray coating. The nanocellulose coated membrane surface was first infrared-dried to a water content of $\sim 10\%$ driers and then the web was thermally annealed for 10 min at a surface temperature of 80 $^{\circ}\text{C}$ to further promote the physical cross-linking between CNF and T-CNF and to ensure the PEI-induced anchoring.

Chemically crosslinked coating on PES membranes

For *paper II*, T-CNF 1 wt% was stirred for 24 h and then sonicated for 10 min at 75% amplitude. PVA powder was added until it reached a concentration of 0.5 wt%. The suspension was stirred and heated to 60 $^{\circ}\text{C}$, then cast coated on the PES membrane at a speed of 5 mm s^{-1} and a gap distance of 100 μm using an automatic film applicator (Elcometer 4340 motorised). The membrane was immersed in acidic glutaraldehyde (GA) solution (5 wt%, pH 2 as set by 1 N HCl) for 1 s and then dried at 70 $^{\circ}\text{C}$ for 20 min. Finally, the membrane was rinsed with de-ionized (DI) water.

Surface impregnation of non-woven cellulose fabrics

For *paper III*, the non-woven cellulose fabrics were cast coated with 1% CNC, T-CNF, or ChNC suspensions. The coating parameters were optimized based on the flux values and the stability of the modification, resulting in 40 mm s^{-1} coated speed and 150 μm gap distance as the best results. Next, the coated fabrics were air-dried for 24 h, and lastly dried for 20 min at 100 $^{\circ}\text{C}$ to ensure binding between the nanocrystals/nanofibrils and the cellulose non-woven fabrics.

2.3 Characterization methods

Morphology, cross-section imaging and coating thickness by Scanning Electron Microscopy (SEM)

For papers I–III, scanning electron microscopy (SEM) (JEOL 7000, acceleration voltage of 3 kV) was used for the characterization of the morphology and cross-section of the samples. The specimens were previously coated with a thin gold layer prior to the visualization using a JEOL JFC-1200 Fine coater at 10 mA for 80 s to promote conductivity.

For paper V, the coating thickness was measured from the cross-section using a Zeiss Merlin field emission SEM (Zeiss International, acceleration voltage 2kV). The samples were sputtered coated (EM ACE200, Leica, Germany) with 5nm of Au/Pd.

Surface roughness by Atomic Force Microscopy (AFM)

For paper I, II, and V, the sample preparation consisted of attaching the samples to metal plugs with double-sided tape and were probed with standard TESPA-V₂ silicon nitride tips (Bruker, USA), with spring constant of $k=40 \text{ Nm}^{-1}$. The imaging was done in tapping mode using a Multimode Nanoscope V (Bruker, USA) atomic force microscope. Data related to height, amplitude, and phase images were recorded and processed using the NanoScope Analysis 1.5 (Bruker, USA) software. The roughness of the samples was measured from the height images, from 10 randomly selected sections, each one with an average area of $0.3 \text{ }\mu\text{m}^2$.

Interfacial anchoring of the coating to the substrate by Quartz crystal microbalance with dissipation (QCM-D)

For paper V, adsorption of T-CNF with and without the anchoring polymer (b-PEI) on PES was studied by monitoring the changes in resonance frequency (Δf) and dissipation energy (ΔD) as functions of time. PES surfaces were prepared as Ultrathin films for interfacial anchoring experiments on piezoelectric AT-cut SiO₂-coated QCM-D sensor surfaces (Biolin Scientific, Gothenburg, Sweden) with a fundamental resonance frequency (f_0) of 5 MHz, and sensitivity constant (C) of $0.177 \text{ mg m}^{-2} \text{ Hz}^{-1}$. Sensors were rinsed with Milli-Q water (Millipore Corporation, Molsheim, France), dried with nitrogen gas and cleaned using UV/ozone treatment (Bioforce Nanosciences, CA) for 10 min. PES surfaces were prepared by dissolving 0.5 wt% of PES membrane

in dichloromethane. PES solutions were spin coated (WS-400 BZ-6NPP-Lite, Laurell Technologies, 6000 rpm for 1 min) on cleaned SiO₂ sensor surfaces and dried at 80 °C for 10 min. Prior to the measurements, the surfaces were stabilized in a desiccator for at least 30 min before being conditioned in Milli-Q water for 10 min until no changes in Δf and ΔD were observed. Water was switched to 0.1 wt% b-PEI solution, and Δf and ΔD were monitored for 20 min followed by Milli-Q water rinsing. Then, 0.15 wt% T-CNF solution was introduced to the QCM-D chamber and after adsorption stabilization. Finally, the system was rinsed with Milli-Q water. Each solution was passed through the QCM-D chamber with a pumping speed of 0.1 mL min⁻¹. Adsorption experiments without b-PEI were carried out by pumping Milli-Q water through the chamber instead of b-PEI. Data presented is acquired using the third overtone (15 MHz, $f_0 = 5$ MHz, $n = 3$).

Permeance and flux

For *papers I–III*, the flux and permeance of the samples were measured by filtering deionized water with a constant pressure of 0.2 bar at 20 °C for 1 h, using a Convergence Inspector Titan equipment. The active filtration area of the membrane was 0.004 m².

For *paper V*, the permeance of the membranes was measured using a stirred cell (Amicon®) in cross-flow filtration conditions. The solutions used to measure the permeance were 0.9% NaCl and 0.1% Cytochrome C in 0.9% NaCl. Also, to test the mechanical durability and integrity of the coated membranes in water filtration, a cross-flow filtration cell (CF042P, Sterlitech, Kent, USA) with an active filtration area of 4200 mm² was used. Water permeance was measured with various feed flow rates (8.5–17.2 L min⁻¹), cross-flow velocities (1.6–3.2 m s⁻¹) and filtration pressures (0.25–1 MPa) at constant temperature of 21 °C with deionized water. Filtration time was 1 h and the volumes of permeates varied from 0.1 to 1.2 L.

Air permeance

For *paper V*, the integrity of the coating layer was assessed by measuring the air permeance (air permeance tester, Lorentzen & Wettre, Sweden) following the Bendtsen method in the cross-direction and machine direction from at least six different locations of each trial point.

Contact angle measurements

For *papers I, II III*, and *V*, the wettability of the samples was measured via the sessile drop technique and using a CAM200 optical contact angle meter from KSV instruments, equipped with a Basler A602f camera (or Attension Theta Optical Tensiometer, Biolin Scientific, Finland in the case of *paper V*). Measurements were taken three times for each material and the contact angle value was recorded at 0.3 s after the droplet reached the surface. The environmental conditions of the test were 23 °C and a relative humidity (RH) of $40 \pm 5\%$ RH.

ζ-potential

For *papers I, II* and *V*, the surface charge of the samples on PES substrates was defined by measuring the ζ-potential as a function of the pH using a SurPASS electrokinetic analyzer (Anton Paar, Graz, Austria) from the streaming current. An adjustable gap cell, at a gap width of 150 μm, was used. The electrolyte solution used was 1 mmol L⁻¹ KCl, and the pH was controlled by titrating with 0.05 mol L⁻¹ HCl and KOH.

For *paper III*, the surface charge of the samples on non-woven cellulose substrates was measured via electrophoretic light scattering ((Zetasizer Nano ZS) using the Surface Zeta Potential Cell (ZEN 1020) from Malvern. All measurements were done at 25 °C using 10 mM KCl(aq) solution with a pH of 7.0, adjusted using 1 M KOH or 1 M HCl. The tracers used were 0.5 wt% poly(acrylic acid) (450 kDa) for negatively charged samples, and 0.5 wt% polyethylenimine (600 Da) for positively charged samples.

Pore size

For *papers I* and *II*, a feed solution consisting of Dextran (50000 Da and 150000 Da, Sigma) and PEG (634 kDa, PolymerLabs) polymer standards was used to obtain the rejection of polymer molecules as a function of their molecular weights. The standard solutions used had a cumulative concentration of 1 g L⁻¹. The standard solution was filtered through the membranes in a dead-end cell at 0.2 bar. Gel permeation chromatography (Viscotek TDA302) was used to analyze the fraction of the molecular weight of each component in the filtrate that passed through the membrane.

For *papers I* and *II*, the specific surface area and the average pore size diameter in the dry state were determined from nitrogen adsorption measurements at 77 K using Brunauer–Emmett–Teller (BET) and Barrett-Joyner-Halenda (BJH)

models, respectively. The measurements were performed using a Micromeritics ASAP 2000 instrument and the samples were degassed at 70 °C for 14 h in dry N₂ prior to the measurements.

For *paper III*, the maximum pore size was determined following the ASTM F316-03 Standard test methods for pore size characteristics of membrane filters by bubble point and mean flow pore test. Previous to the test, the samples were conditioned by submerging them in DI water for one minute. The test was performed using a Sterilitech in dead-end cell mode.

Functional groups on the surfaces by X-ray Photoelectron Spectroscopy (XPS)

For *papers I and II*, X-ray photoelectron spectroscopy (XPS) was used to characterize the functional groups on the surface of the samples. The surface of the samples was cleaned using Ar-clusters (1000 atoms, 6000 eV, 1 mm raster size) for 60 s. The analysis was performed using a Nexsa XPS system (Thermo-Fisher) with a radiation source gun-type Al K α operating at 72 W and a pass energy of 200 eV, a spot size of 400 μ m, “Standard Lens Mode”, CAE Analyzer Mode, an energy step size of 0.1 eV for the survey spectrum, and integrated flood gun. The high-resolution C 1s spectrum was acquired after 10 passes at a pass energy of 50 eV and fitted using Thermo Avantage v5.9914, Build 06617 with Smart background and Simplex Fitting algorithm using Gauss-Lorentz Product.

For *paper V*, the same instrument was used, but in this case the sulfur (at a binding energy of 167 eV) originating from PES was used as a marker to follow the coating evenness and coverage. Also, the amount of nitrogen, which is part of the b-PEI anchoring polymer, was used to evince both the attachment of the anchoring polymer and the nanocellulose coating. The analysis was performed with an energy step size of 1 eV for the survey spectrum (20 passes), and integrated flood gun. The high-resolution spectra (step size 0.1 eV) of the single elements were acquired with 20 passes at pass energies of 50 eV. The cumulated data presented represents the average of the measurements performed at 16 points covering an area of 8.7 mm².

Dye adsorption/rejection by Ultraviolet-visible spectrophotometry (UV-vis)

For *paper II*, the adsorption/rejection of charged dyes by the membranes was characterized by submerging them in a Petri dish containing 2 mg L⁻¹ solution of Victoria Blue (VB) (positively charged at pH 5.6) or Methyl Orange (MO) (negatively charged at pH 5.8) for 6 h. Later, UV-vis (Genesys 150) was used to analyze the solution at a wavelength of 450 nm for MO and 610 nm for VB.

Protein rejection performance

For *paper V*, the protein rejection performance was studied using a solution of 0.1% Cytochrome C in 0.9% NaCl using a stirred cell (Amicon®) in cross-flow filtration conditions. Cytochrome C is a protein commonly used for testing the ultrafiltration property of molecular weight sieving. The protein concentrations of the initial solution and the collected filtrates were determined by UV spectrometry (Infinite 200 PRO, Tecan, Männedorf, Switzerland) at a wavelength of 280 nm.

Size exclusion performance

For *paper III*, the size exclusion performance of the samples on non-woven cellulose substrates was assessed by studying the particle retention performance. For this, 20 mL suspensions of PS latex spheres (50 nm, 500 nm, and 2 µm) were passed through the samples at a constant pressure of 0.2 bar using a Sterilitech in dead-end cell mode. The intensities of light scattered by the feed and permeate solutions were measured via Dynamic Light Scattering (DLS) using the Zetasizer Nano ZS from Malvern Instruments. The parameter called “derived counted rate” was used to find the difference on concentration between the feed and permeate, and thus calculate the rejection rate.

Rejection performance based on size exclusion and charge

For *paper V*, sieving curves and the MWCO of the membranes were defined by passing polystyrene sulfonates (PSS, ζ-potential of 63 mV at pH 7⁵⁵, mixture of 2, 4, 10, 29 and 64 kDa molecules) and dextrans (neutral, a mixture of 4, 8 and 35 kDa molecules), of known concentrations through the membranes. The filtered amount was 9.5 mL at 0.4 MPa pressure using 25 mm diameter membrane specimens. Filtrates were collected and analyzed by combined high-performance liquid chromatography-size exclusion chromatography (HPLC-SEC, UltiMate 3000 system from ThermoFisher). The molecular weight distribution yielded by the refractive index signal of the

filtrate was normalized against the signal and the corresponding distribution for the applied mixture. This ratio is called sieving curve giving the molecular weight cut off (MWCO) that were recorded at 80, 90 and 95% rejection levels.

Mechanical tests

For *papers I–III*, the tensile properties of the samples were measured using an Instron 5966 Dual Column Tabletop Testing System equipped with a 100 N load cell. The samples were cut as rectangular strips of 10 mm × 100 mm from the membranes. Prior to the test, the samples were conditioned for 40 h at 50 ± 5% RH and 23 ± 2 °C. The tensile test was performed at a speed of 25 mm min⁻¹ until failure.

Tensile tests were also performed using the same parameter settings under wet conditions using a BioPuls temperature-controlled chamber. Samples were pre-conditioned by placing them underwater, held by the grips, for 5 min before starting the test. The temperature of the water bath was kept at 25 ± 2 °C.

Organic fouling resistance (OFR)

Organic fouling resistance was assessed using Bovine serum albumin (BSA) as model protein for all the experiments.

OFR by Quartz crystal microbalance with dissipation (QCM-D)

Direct assessment of BSA adsorption on different surfaces was performed using a Quartz Crystal Microbalance with Dissipation monitoring (QCM-D E4, Q-sense AB). SiO₂ sensor crystals (Biolin Scientific AB) were rinsed with MilliQ water, dried with nitrogen gas and cleaned with a UV/ozone treatment for 10 min. A cationic anchoring polymer was adsorbed on the sensor crystals by immersing the crystals in 0.1% PEI solution for 30 min. The crystals were then washed with Milli-Q water and dried with nitrogen gas.

For *papers I and V*, a 200 µl droplet of CNC or T-CNF suspension at 0.15% consistency, PES or b-PEI were spin-coated (WS-400 BZ-6NPP-Lite, Laurell Technologies Corporation, 3000 rpm, 1 min) on the sensor and dried in an oven (10 min, 80 °C). The CNC or T-CNF coated crystals were kept in 0.9% NaCl (pH 4.63) overnight before the adsorption experiments in the QCM-D measurement cell. A continuous flow (0.1 mL min⁻¹) of 0.9% NaCl was

pumped over the crystal in the QCM-D cell for 5–10 min. The solution was exchanged to 0.1% BSA in 0.9% NaCl solution (pH 6.1) and the changes in frequency and dissipation were followed for 1 h. Finally, the solution was exchanged back to 0.9% NaCl and rinsed for 5–10 min. The cell temperature was 21 °C. The data presented was acquired using the third overtone (15 MHz, f_0 = fundamental resonance frequency = 5 MHz, n = overtone number = 3).

For *paper II*: 200 μ L of a 0.15 wt% suspension of T-CNF or 0.15 wt% T-CNF/0.075 wt% PVA was spin-coated (WS-400 BZ-6NPP-Lite, Laurell Technologies Corporation, 3000 rpm, 1.5 min) on the sensor. Separately, the pH of a 0.75 wt% GA solution was adjusted to 2 by dropwise addition of 1 N HCl. Afterward, a droplet of this GA solution was placed on the surface and then washed with MilliQ water. The crystals were dried in an oven (20 min, 70 °C). The crosslinked T-CNF and T-CNF/PVA coated crystals were kept in 0.01 M PBS solution overnight before QCM-D measurements, during which a continuous flow (0.1 mL min⁻¹) of PBS (0.01 M) solution was pumped over the crystal in the QCM-D cell for 30 min. The solution was exchanged to 0.1% BSA in PBS (0.01 M), and the changes in frequency dissipation were followed for 1 h. Finally, the solution was changed back to PBS (0.01 M) and the crystal was rinsed for 30 min. The cell temperature was 37 °C. Data presented was acquired using the third overtone (25 MHz, f_0 = fundamental resonance frequency = 5 MHz, n = overtone number = 5).

OFR by Ultraviolet-visible Spectrophotometry (UV-vis)

For *papers I and II*, ultraviolet-visible spectrophotometry (UV-vis) was used to analyze the adsorption of Bovine serum albumin (BSA) on the surface of the samples, with PBS as buffer solution. BSA was dissolved in 0.01 M PBS solution at a concentration of 1 mg mL⁻¹. The membranes were conditioned by keeping them submerged in PBS overnight and then exposed to a continuous flux of BSA solution for 6 h at 37 °C. After that, the membranes were rinsed thrice with PBS, and one last time with 1 wt% sodium dodecyl sulfate (SDS) solution for 1 h at 37 °C under slight shaking (200–300 rpm). The SDS solution used for rinsing the membranes was analyzed using a UV-vis (Genesys 150) at a wavelength of 280 nm.

OFR by Fourier Transform Infrared Microscopy Imaging (FTIR-mapping)

For *paper I*, a Fourier transform infrared microscopy imaging (FTIR-mapping) (PerkinElmer Spotlight 400 FTIR imaging system equipped with a germanium attenuated total reflection crystal) was used to characterize the chemical composition of the surface of samples exposed to a continuous flux of BSA solution for 6 h at 37 °C. The scanned area was $50 \times 50 \mu\text{m}^2$ with a pixel size of $6.25 \mu\text{m}$, 16 scans per pixel, and the spectral resolution was 8 cm^{-1} . The spectrum range scanned was 4000 to 750 cm^{-1} .

OFR by Confocal microscopy

For *paper III*, samples were immersed in BSA solution (not continuous flux as mentioned in section 2.3.11.2). UV-vis was used to analyze the adsorption of BSA on the surface of the samples, with PBS as the buffer solution. BSA was dissolved in 0.01 M PBS solution at a concentration of 1 mg mL^{-1} . The membranes were conditioned by keeping them submerged in PBS overnight and then immersed in the BSA solution for 6 h at 37 °C. After that, the membranes were rinsed thrice with PBS. The samples were stained using a Qubit Protein Assay Kit. The proteins were visualized with a Zeiss LSM 780 Confocal fluorescence microscope (Carl Zeiss MicroImaging GmbH, Oberkochen, Germany). The excitation/emission wavelengths were 485 nm and 592 nm.

Biofouling resistance, bacterial colonization and viability

For *papers I–III*, bacterial colonization and biofilm formation were assessed after the incubation of membrane specimens with bacterial cells on polystyrene 24-well plates. Exponentially growing cultures of *Escherichia coli* (*E. coli*) ATCC 8739 on Nutrient Broth (NB) were diluted to an optical density of 0.0138 at a wavelength of 600 nm (OD_{600}), equivalent to $10^8 \text{ cells mL}^{-1}$. 2 mL of diluted cultures were placed on the surface of the membranes, which were subsequently incubated for 18 h at 37 °C without stirring. After the biofilm assay, the liquid culture was removed and membranes were carefully rinsed with distilled water to remove non-adhered cells.

Biofouling resistance by Scanning Electron Microscopy (SEM)

For *papers I and II*, the adhesion of bacterial cells on the surface of the membranes was visualized by SEM. Cell fixation was carried out in glutaraldehyde 5% (v/v) in 0.2 M sodium cacodylate buffer (pH 7.2) for 1 h at room temperature. The samples were then rinsed in cacodylate buffer and

dehydrated in an ascending ethanol series (25, 50, 70, 90 and 100%) before critical point drying with CO₂ and subsequent observation with SEM.

Bacterial viability by Confocal microscopy

For *papers I and III*, to evaluate bacterial viability, the Live/Dead BacLight Bacterial Viability Kit (Molecular Probes, Invitrogen Detection Technologies, Carlsbad, CA, USA) was used. After bacterial incubation with CNC or T-CNF suspensions for 18 h at 37 °C, cell cultures were stained with 10 µL BacLight stain (a mixture of SYTO 9 and PI in DMSO) according to the manufacturer's recommendations, then incubated in the dark for 15 min at room temperature. All images were acquired using a Leica Microsystems Confocal SP5 fluorescence microscope (Leica Microsystems, Germany). For green fluorescence (SYTO 9), excitation was performed at 488 nm (Ar) and emission was recorded at 500–575 nm. For red fluorescence (PI, dead cells), the excitation/emission wavelengths were 561 nm (He–Ne) and 570–620 nm, respectively.

Bacterial viability by biological studies and AFM

For *paper IV*, bacterial viability, morphology, nanomechanical properties and interaction forces were studied by adding 500 µL of *E. coli* on LB media to the previously sterilized and incubated flasks with nanopolysaccharide films. The flasks were kept under constant agitation at 37 °C. Samples at $t = 0, 24, 48, 72$ and 96 h were taken to determine the UFC/OD₆₀₀ and the slope of the linear regression was calculated for the linear growth phase.

Morphology, nanomechanical properties and interaction forces were assessed by PeakForce quantitative nanomechanical mapping (PFQNM) using a MultiMode AFM (Bruker, Santa Barbara, CA) equipped with the Nanoscope V controller equipped with a MultiMode 8-HR AFM controller with enhanced PeakForce QNM-HR module. AFM samples were prepared under sterile conditions. The control *E. coli* sample was prepared by washing the original cell cultures in PBS 7.0 buffer. The cells were diluted to 1:10 PBS. Afterwards, 500 µL of diluted cells suspension was mounted onto sterilized cleaved mica. The control films and films exposed to bacteria were removed from the flask used for the incubation (containing the bacterial culture after reaching the plateau stage in the growth curve in the case of the ones exposed to *E. coli*), and they were rinsed with new LB media to remove any bacteria that was not attached to the surface. Then the film was placed over a sterile surface and gently dried with a sterile tissue. Double sided taped was attached

to the metallic sample holder and the sample was placed over it. The sample was kept in sterile conditions until its analysis.

3. Functionalized nanopolysaccharide coatings to enhance commercially available membranes and non-woven fabrics

Nanopolysaccharides can be used to functionalize surfaces for use in separation processes by modifying the surface charge, the hydrophilicity or the roughness. These changes result in different effects on the performance of the pristine surface, such as size exclusion, electrostatic interactions, antifouling, and antibacterial properties. Furthermore, surface modification by coating, assures a homogeneous distribution of the nanoparticles and is considered easy and scalable process. In this chapter, we propose three coating approaches; (i) a simple layer-by-layer coating⁵⁶, (ii) a chemically crosslinked coating⁵⁷, and (iii) a high-flux coating⁵⁴; and the different functionalities imparted by the surface modification are explained.

Simple layer-by-layer waterborne coatings for antifouling purposes

In *paper I* we presented a comparative analysis between two waterborne coatings applied by cast coating, using the layer-by-layer deposition technique on commercialized PES membranes, originally intended to be for single-use pharmaceutical separation applications. Membranes that are used to separate e.g. biological samples from their preparation media or for the sterile filtration of culture media and buffers, have organic materials (e.g. biomacromolecules including BSA, natural organic matter) and biofoulants (e.g. microorganisms) as typical foulants^{3,7,58}. The morphology, membrane performance, as well as the antifouling performance of the nanocellulose coated membranes was studied.

The modification method employed was the layer-by-layer deposition technique, by cast and dip coating. Poly(allylamine) hydrochloride (PAHCl), a weak polyelectrolyte, was used as the anchoring agent between the negatively charged PES membranes and the negatively charged nanocelluloses (CNC and T-CNF). The electrostatic interactions between the three layers guaranteed a robust adhesion and a distinct stability of the coating (Figure 3.1).

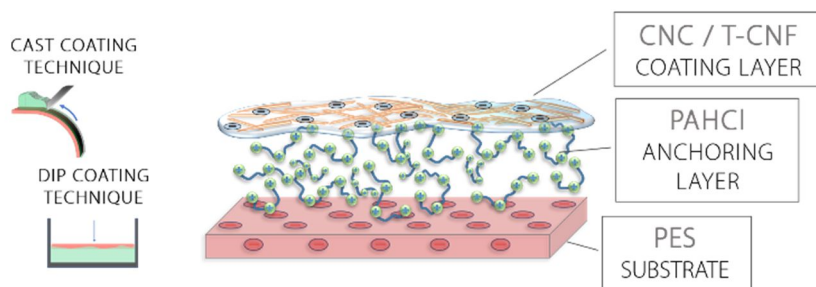


Figure 3.1 Schematic representation of the layer-by-layer coatings proposed in paper I⁵⁶.

SEM images showed that surfaces were homogeneously coated and nanocellulose top-layers of either CNC or T-CNF of $0.26 \pm 0.01 \mu\text{m}$ and $0.34 \pm 0.01 \mu\text{m}$ thickness, respectively, were formed. The coating layer provided a smoother surface compared to the uncoated one as demonstrated by the surface roughness measurements. The nanoscale coating layer did not significantly affect the flux performance of the original PES membrane; nevertheless, it shifted its performance from the microfiltration regime towards the ultrafiltration regime, thus improving its size-exclusion properties. The CNC and T-CNF coatings also had a clear impact on the wettability, increasing the membrane hydrophilicity by up to 52%. The hydrophilic coating facilitates the formation of a hydration layer on the surface of the membrane, which acts as a physical and energetic barrier, preventing the adsorption of protein and other foulants on the surface³⁹. Both coatings had a clear impact on the surface charge of the membranes. The ζ -streaming potential for the coated membranes was lower compared to the uncoated ones. This indicated the presence of an abundance of negatively charged carboxylate or sulfate half-ester groups, respectively, in addition to hydroxyl and aldehyde groups for the T-CNF and CNC coatings, on the surface of the PES membranes. The addition of coatings, and especially CNC coatings, positively influenced the tensile strength and Young's modulus of the membranes. The elongation at break under both dry and wet conditions was decreased.

During the study of organic fouling resistance, CNC and T-CNF coated membranes showed a relative reduction of BSA adhesion of 41% and 49%, respectively, compared to the uncoated PES membranes. This was attributed to the abundant hydroxyl and carboxyl groups on the surface of the cellulose nanofibrils or nanocrystals, which allowed a layer of water to bind to the surface, preventing the adhesion of BSA. In the same way, ζ -streaming potential results also confirmed that having a more negatively charge surface generates stronger repulsion forces between the surface and foulants. The

increases in both hydrophilicity and surface charge suppressed non-specific interactions with proteins, preventing the attachment of negatively charged foulants, such as BSA, onto the membrane surface^{58,59}. Furthermore, having a protective layer on top of the membrane surface reduces the fouling inside the pores, therefore minimizing pore blockage or pore adsorption of the membrane⁶⁰.

Chemically crosslinked coatings with electrostatic selectivity and antifouling properties

Although using nanocellulose on membranes has multiple advantages, it is prone to swelling in aqueous media and can present poor mechanical stability in humid environments due to its intrinsic hygroscopicity⁶¹. This is a major disadvantage when it comes to applications such as membranes exposed to liquid media. *Paper II* tackled this issue, and in addition, we provided the original MF PES membranes with a separation range in the UF regime, exceptional antifouling properties, and electrostatic selectivity.

We developed a T-CNF coating formulation anchored and stabilized by chemically crosslinking poly(vinyl) alcohol (PVA), using glutaraldehyde (GA) in acidic conditions as a crosslinker, in order to prevent the coating from swelling and dissolving in an aqueous media⁶². The MF PES substrate, was coated with T-CNF, but also, it was crosslinked it with PVA for several reasons. PVA promoted the interfacial adhesion between hydrophobic PES and hydrophilic T-CNF^{63,64}, thus acting as an anchoring polymer. Furthermore, the reaction of PVA with the T-CNF formed ester bonds⁶¹, reducing possible swelling and improving the selectivity of the membranes⁶⁵. To improve the stability and the mechanical properties as well as to provide insolubility in aqueous media, GA was used for additional crosslinking^{66,67}. The generated intra and intermolecular interactions between the hydroxyl groups of PVA and T-CNF, and the aldehyde groups of GA. This reaction is possible in presence of strong acids such as HCl, which catalyze the reaction^{62,65,66,68,69} and further drive the esterification reaction between T-CNF and PVA⁶¹ (see Figure 3.2).

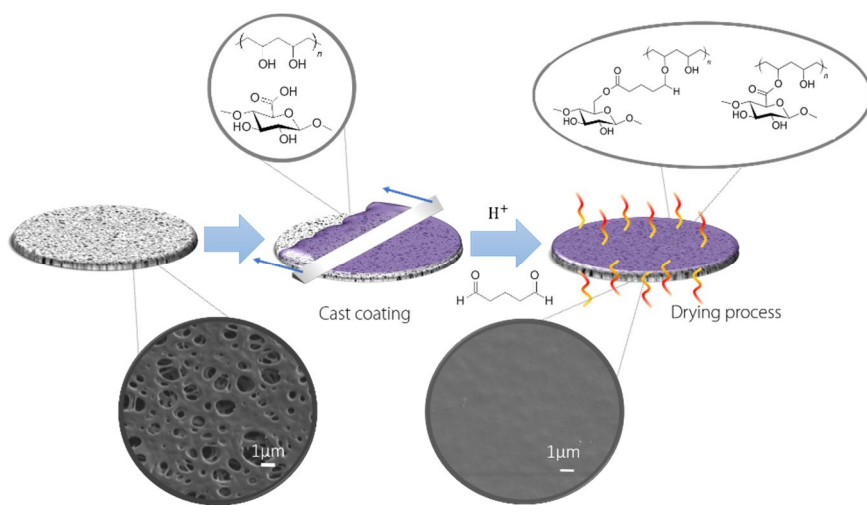


Figure 3.2 Conceptual schematic illustration of the chemically crosslinked coating proposed. Taken from Aguilar-Sánchez et al.⁵⁷ and adapted with permission of the Royal Chemistry Society.

SEM images confirmed that the coating layer was deposited homogeneously on the PES membrane. The AFM images showed a uniform, nanotextured T-CNF/PVA layer on the substrate; that had less than half of the roughness value compared to the uncoated membrane (see Figure 3.3). The surface charge was more negative along a pH range from 2 to 10 due to the abundance of hydroxyl and aldehyde groups on the surface of the modified membranes; therefore, the coated membranes can be used in applications involving a wide pH range. The XPS data showed no peak attributed to -COOH , confirming that the carboxyl group of the T-CNF reacted with the alcohol group of the PVA, forming covalent ester bonds during the crosslinking. Furthermore, the coating did not improve wettability, since the hydroxyl groups of the cellulose were crosslinked with the aldehyde groups of GA while also forming hydrogen bonds with the -OH groups in PVA.

The original PES substrates with a nominal pore size of $0.2\ \mu\text{m}$ (MF regime) were converted to UF membranes after applying the coating, showing a 90% rejection of 30 nm particles. Nevertheless, the nanoscaled coating had a minor effect on permeance, reducing the flux by only 4%. The addition of the coating also improved dye adsorption/rejection, adsorbing 97% of VB dye from the filtered solution. This confirms the membrane selectivity to charged contaminants. Lastly, the mechanical properties were improved in both dry and wet conditions, confirming the stability of the modification in an aqueous solution.

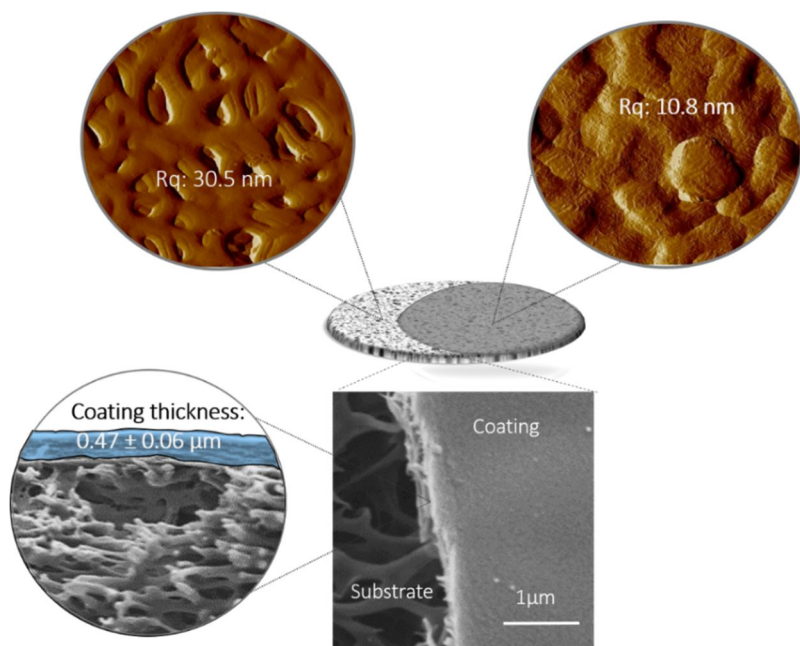


Figure 3.3 SEM and AFM images of the T-CNF/PVA coated membrane.

QCM-D results confirmed that T-CNF/PVA coatings were highly resistant to organic foulants such as BSA. In addition, the coated membranes exposed to regular use had 75% less relative adhesion of BSA on the surface compared to the uncoated PES membranes. This was attributed to the hydroxyl groups on the surface of T-CNF, which allowed a layer of water to bind to the surface, staying in between the coating and the protein and therefore preventing the adhesion of the BSA.

High-flux coatings for selective particle rejection and antifouling purposes

Effective and sustainable alternatives to the currently available MF membranes used for water recycling in domestic and industrial effluents are necessary. Non-woven fabrics are efficient in the MF range, and cellulose-derived membranes are available on the market. MF membranes have the biggest pore sizes; hence they provide high flux. A surface modification on non-woven fabric within the MF range is equivalent to a modification of its fibers, giving new properties to the coated fabric without reducing drastically the pore size or the flux. Fully bio-based substrates and coatings were compared in *paper III*.

The non-woven cellulose fabrics were impregnated by cast coating with CNC, T-CNF, or ChNC suspensions (see Figure 3.4). In general, the nanocrystals/nanofibrils suspensions were successfully and homogeneously impregnated on the surface of the fibers. Impregnation of the nanocrystals onto the surface of the non-woven fibers was desirable to ensure their surface functionality and accessibility. After coating, build-up and nanocrystal/nanofibril films were observed in the junctions (crossover) of the non-woven fibers, especially in the case of T-CNF. A nanotextured surface was achieved on the surface of the fibers after coating them with nanocrystals/nanofibrils, compared to the smooth surface of the unmodified fibers.

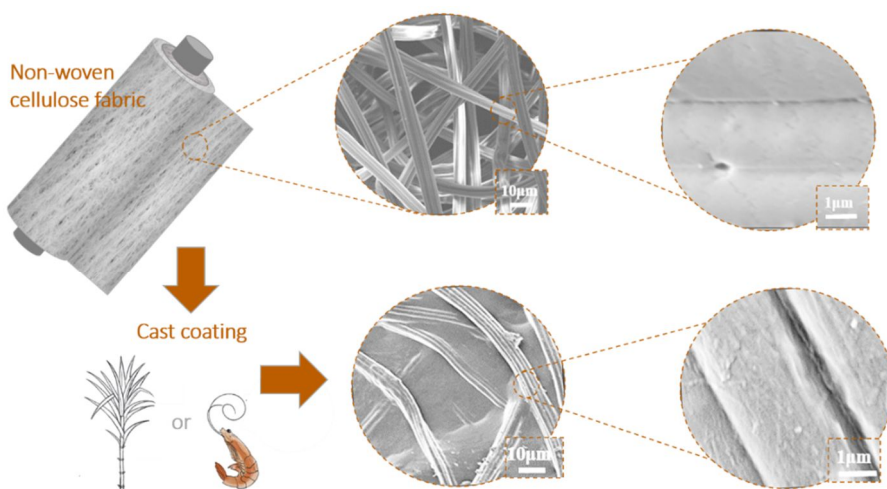


Figure 3.4 SEM of the impregnated and pristine cellulose fabrics.

Impregnating the fabrics with different types of nanoparticles suspensions caused major changes in their permeability, wettability, surface charge, and particle rejection performance without drastic changes in the pore size. The cellulose non-woven fabrics were modified from being hydrophobic (contact angle of $106 \pm 3^\circ$) to being hydrophilic in the cases of CNC and T-CNF (68 ± 4 and $49 \pm 1^\circ$, respectively) due to the abundant hydroxyl groups and carboxyl groups on T-CNF; and extremely hydrophilic for ChNC (0°), due to the nitrogenated groups in their structure^{3,8,9,56}. At neutral pH, all the fabrics were negatively charged, except for ChNC, which possessed amino groups due to acid-hydrolysis-induced deacetylation. The protonation of these amine groups makes the surface overall less negative or even positively charged⁵¹. Both

CNC and ChNC improved the permeance of the original fabric (9 and 2% higher permeance, respectively), while T-CNF decreased permeance by 43% by forming a web-like structure within the pores of the fabric. Particle retention experiments showed that T-CNF-impregnated fabrics can be effectively used for microplastics removal since the 2 μm sized PS beads were retained on the surface of the film-like structure formed by the coating, as well as attached to the fibers. The other samples showed lower rejection since the beads were only attached to the surface of the fibers, without the possibility of being retained by a layer of coating. The CNC-impregnated samples exhibited the best separation performance when filtering 500 nm particles (bacteria and virus range), with a 93% filtration efficiency. SEM images confirmed that when the size of the particles is comparable or smaller than the pore size, the particles can flow into the membrane and get retained in settling zones deep in the membrane. Furthermore, the non-uniform structure of non-woven fabrics causes a tortuous flow path⁷⁰, which in turn causes multiple mechanisms by which particles are retained onto the membrane. None of the samples efficiently reject 50 nm particles, and the SEM images of used membranes showed no retention of these particles on the surface, confirming that they could travel freely through the membrane (Figure 3.5).

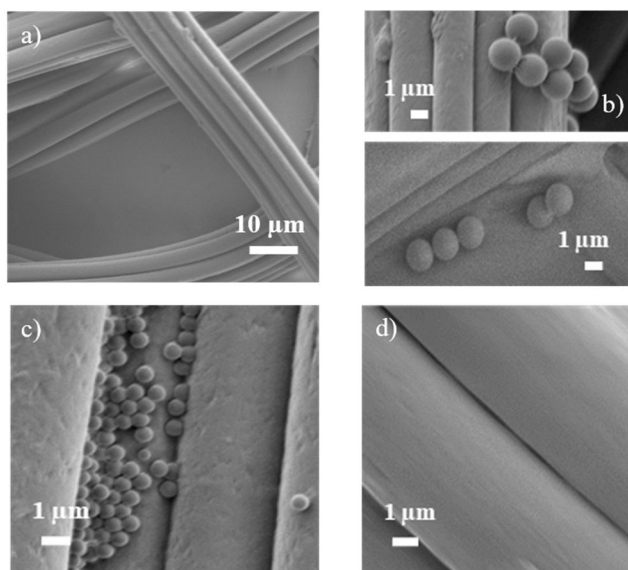


Figure 3.5 SEM images of (a) “film-like” structure between fibers on T-CNF-impregnated fabrics, (b) 2 μm particles retained on T-CNF-impregnated fabrics, (c) 500 nm particles retained on CNC-impregnated fabrics, and (d) pristine fabric after exposure to 50 nm particles.

In addition, at pH 7, adsorption of BSA was highest on ChNC-impregnated nonwoven fabrics. The large BSA adsorption to positively charged surfaces, such as ChNC-impregnated fabrics, can be attributed to the strong electrostatic interactions between chitin and BSA, the latter being negatively charged at neutral pH. These values were followed by the unmodified fabrics and the CNC-impregnated fabrics. The lowest adsorption was observed on the T-CNF impregnated fabrics. It is important to emphasize that the pH conditions in which antifouling performance is tested have a dominant influence over the results since BSA is negatively charged at neutral pH and positively charged under acidic conditions (isoelectric point (IEP) = 4.5–5.0)^{71–77}.

4. Revealing the effect of nanopolysaccharide-based coatings on bacterial viability

Bacteria are single-celled microbes that, in Nature, are found as a single bacterium in a medium or as biofilms over a surface. More than 99% of bacteria live attached to surfaces as biofilms, often leading to biofouling, which in a lot of cases can cause detrimental effects in humans and industrial settings³⁶. Bacterial attachment and biofilm formation are complex, still poorly understood phenomena, which depend on several factors, including the physicochemical properties of the surface, temperature, pH, the availability of nutrients, and the type of strain⁵⁴. To tailor surfaces and materials that can tune bacterial growth or cause their death, it is critical to understand how material properties affect the microbe–surface interactions²⁷. In general, there are three main strategies to functionalize a surface in a way that controls bacterial spreading. These are antibiofouling, leaching or biocide release, and a non-leaching/contact-active antibacterial approach.

In *paper I*, the antibiofouling performance of uncoated PES was compared to those of CNC-, and T-CNF-coated PES. It was possible to observe *E. coli* cells attached to the surface of the PES membrane with a low amount of extracellular matrix surrounding the cells, indicating low biofilm formation. The CNC-coated membranes presented an important development of the extracellular matrix and biofilm formation upon contact with *E. coli* cultures, compared to the uncoated membranes. In this case, bacteria were not only using the CNC coating to enhance their adhesion to the surface, but also degraded the coating. *E. coli* exhibits a certain cellulolytic effect and can degrade cellulose, metabolizing it in ethanol and hydrogen and, presumably, using it as carbon source promoting their growth^{78–80}. On the contrary, membranes coated with T-CNF exhibited high resistance to bacterial colonization and biofilm formation. The antibiofouling characteristics of T-CNF could be attributed to the carboxyl groups located on the surface of the oxidized cellulose nanofibrils and, thus, to the acidic environment that carboxyl groups generate⁸¹ since the pH of the bacterial culture shifted from 7.2 to approximately 4.8 after 18 h of incubation of the *E. coli* inoculum with the T-CNF coated membranes. This pronounced variation of the pH was not observed after incubating the cell culture with the uncoated membranes or with the CNC-coated membranes. Microorganisms have certain general physiological requirements for survival and growth, which include an appropriate pH. High acidity or alkalinity can effectively limit the growth and

survival of microorganisms, and the variation observed in our experiments agrees with the limiting growth range for many organisms, including *E. coli*^{82,83}. Live/dead assessment was done by staining the bacterial cells to confirm the effect of T-CNF on *E. coli*. The bacterial viability was compromised after incubation of the cells with T-CNF suspension, thus demonstrating the antibacterial effect of T-CNF. Figure 4.1 shows a summary of the results for the T-CNF coated membranes.

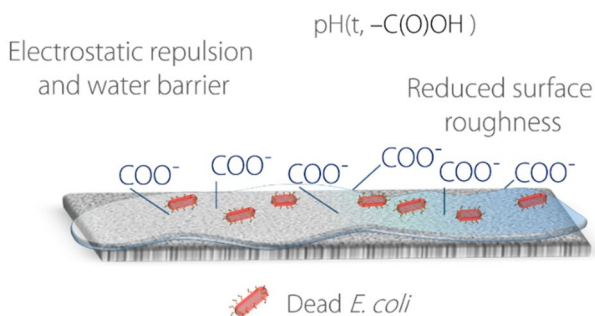
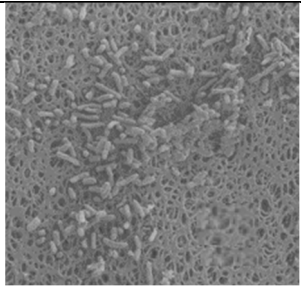
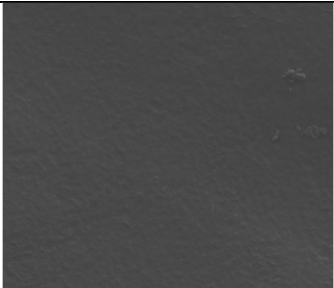
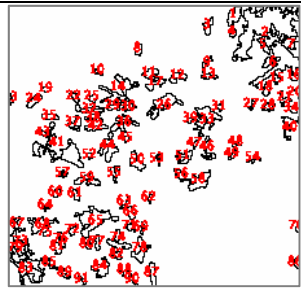
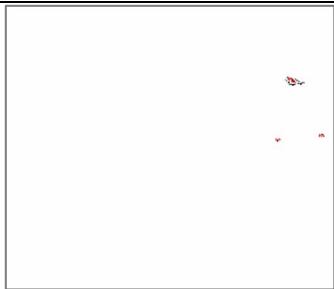


Figure 4.1 Schematic representation of T-CNF coating effect over *E. coli*. Taken from Aguilar-Sánchez et al.⁵⁶ and adapted with permission of Elsevier.

Paper II explored the effect of chemically crosslinked T-CNF/PVA coatings on biofilm formation, and compared it with that on uncoated PES membranes. Membranes coated with T-CNF/PVA exhibited higher resistance to bacterial colonization and biofilm formation not only than pristine PES membranes (Table 4.1), but also than the T-CNF-coated membranes described in *paper I*. The combination of repulsive forces between the negatively charged surface and the *E. coli*, and a reduction in surface roughness, prevented the adhesion of the bacterial appendages to the surface. In addition, aldehyde groups can strongly associate with the outer layers of bacterial cells, more specifically, the unprotonated amines on the cell surface, damaging the bacterial cell wall and cytoplasmic membrane, leading to the death of the bacterial cells^{84,85}.

Table 4.1 Quantification of bacteria using Image J. Taken from Aguilar-Sánchez et al.⁵⁷ with permission of Royal Chemistry Society.

Samples	PES substrate	PES substrate + TCNF/PVA membrane
SEM		
Image J visualization		
Bacterial coverage area (%)	10.2	0.04

The coatings described in *paper III* displayed important resistance towards *E. coli* colonization (see Figure 4.2), except ChNC impregnated samples, which showed slightly higher microbial attachment than unmodified cellulose non-woven fabrics attributed to the surface charge at pH 7. The *E. coli* outer membrane is negatively charged⁸⁶, and it was attracted to the positive charge of ChNC, while being repulsed by CNC and T-CNF. Furthermore, the bacterial viability tests showed that neither the pristine nor the CNC-impregnated fabrics significantly impaired the bacterial cells. In contrast, T-CNF- and ChNC-impregnated nonwoven fabrics reduced the viability of the cells, showing an antibacterial effect that was more evident for ChNC. As aforementioned, the presence of carboxyl groups in T-CNF provide enough antibacterial activity by lowering the pH of the environment, making it hostile for bacterial survival^{56,83,87}. In the case of the ChNC, the crystals structure have NH_3^+ groups, formed during the hydrolysis process, which interact with

the negatively charged cell surface of bacteria ^{10,88}, presumably by competing with Ca^{2+} for electronegative sites on the membrane surface ^{13,49}.

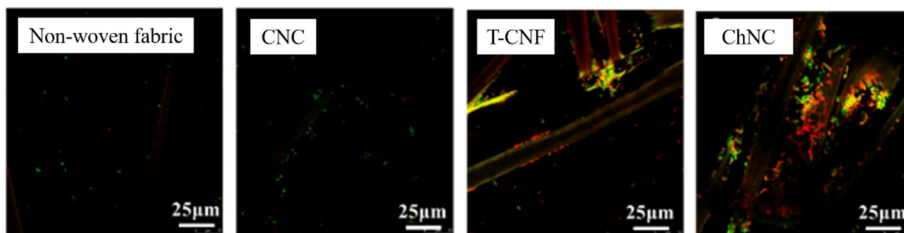


Figure 4.2 Confocal microscopy micrographs showing *E. coli* colonization and viability on the different surfaces studied. Taken from Jalvo et al.⁵⁴ and adapted with permission of MDPI.

Paper IV revealed the long-term effects of CNC, T-CNF, L-CNC and ChNC on *E. coli*, both when the polysaccharide was exposed to a nutrient-rich media, as well as when it is in direct contact with films prepared using the different nanopolysaccharides. The films were sterilized prior the study to assure that no cross-contamination. Afterwards, *E. coli* was added to the different types of samples. Results were categorized into two: (i) the observations of the bacteria growing in the LB medium containing only *E. coli* or *E. coli* and a nanopolysaccharide film, and (ii) the surface interactions between the nanopolysaccharide film surface and the bacteria adhered to it (see Figure 4.3).

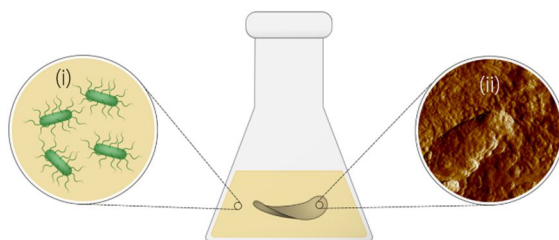


Figure 4.3 Schematic representation of the two types of results obtained and analyzed during this study; (i) bacterial growth in the LB media, and (ii) surface interactions between the films and the bacteria on top of them.

Firstly, the bacterial growth curve in the LB medium was defined through optical density OD_{600} from 0 to 96 h, at dynamic conditions. In parallel, the CFU was determined for each time point. The changes in CFU per volume per OD_{600} at the end of the linear growth curve indicated that none of the films were toxic to the *E. coli* growing in the LB media. Nevertheless, the films had

different cytostatic effects, that is to say effects of the rate of bacterial growth. The cytostatic effect was determined by estimating the growth rate, or slope of the linear regression of the change in OD₆₀₀ over time, and different film compositions affected the bacteria in different ways. T-CNF, L-CNC and ChNC showed a cytostatic effect. CNC-exposed bacteria grew normally, which is aligned with the results gathered before^{54,56}. In general, bacteria are expected to degrade cellulose, metabolizing it into ethanol and hydrogen, and using it as carbon source to promote their growth^{78–80}, and this seemed to be the case for CNC. In the case of T-CNF, the cytostatic effect observed demonstrated that the carboxylic groups in T-CNF have a major impact on the media even if the bacterial cells are not in direct contact with it. This is aligned with our previous studies where the carboxylic groups had an impact on the media, making it hostile to bacterial life. A different effect is expected from positively charged ChNC films, which attract the bacteria by electrostatic interaction. The negatively charged carbohydrates, lipids, and proteins on the surface of the bacterial cells are attracted to the $-\text{NH}_3^+$ groups on the deacetylated structural units of ChNC. Nevertheless, $-\text{NH}_3^+$ groups compete with Ca^{2+} for electronegative sites on the bacterial membrane surface, resulting in bacterial impairment. In the case of L-CNC, it was expected that the phenolic compounds in lignin as well as the carbonyl and carboxylic acid functional groups, can damage the bacterial membrane and suppress biofilm formation when in direct contact⁸⁹, but not necessarily in the LB media.

We defined the interactions between the films and the bacteria adhered to them using AFM imaging and PFQNM technique. The *E. coli* cells attached to the CNC surfaces did not show damage or crack-like features. The cells tended to penetrate under the surface of CNCs during the cell cultivation in LB media, while the *E. coli* cells stayed at the top surface of the T-CNF, L-CNCs and ChNC films. This is consistent with the results of our previous study⁵⁶, where *E. coli* seemed to benefit from and degrade CNC coatings. CNC films seemed to serve as carbon source to the *E. coli*, since the cells were underneath rather than on top of the film. Furthermore, it also aligns with the lack of cytostatic effect mentioned in the previous paragraphs. In addition, AFM imaging revealed that T-CNF, L-CNC and ChNC have a non-leaching/contact-active effect on *E. coli* cells, as damage to their edges was observed. Figure 4.4 shows an example of the peak force error images taken to L-CNC film and *E. coli* exposed to the L-CNC film.

A roughness study was done over the *E. coli* cells on top of the films, being higher for *E. coli* over ChNC > L-CNC > T-CNF. Previous studies have attributed an increase in roughness to the extent of cell damage⁹⁰. Further analysis was done by defining the DMT modulus of the *E. coli* cells and the

adhesion force between the cells and the film surfaces. The highest DMT modulus, ~ 312 GPa, was observed for ChNC, followed by T-CNF ~ 276 GPa, and L-CNC ~ 144 GPa; indicating a major stiffening of the cells exposed to ChNC. The adhesion forces measured between the film surface and the *E. coli* showed that the strongest adhesion force was between ChNC-*E. coli*, then T-CNF-*E. coli* and lastly for L-CNC-*E. coli*. This gives even more evidence that ChNC attract bacteria by electrostatic interactions, then affect them negatively. In the case of L-CNC and T-CNF, bacteria interact with the surfaces via their functional groups.

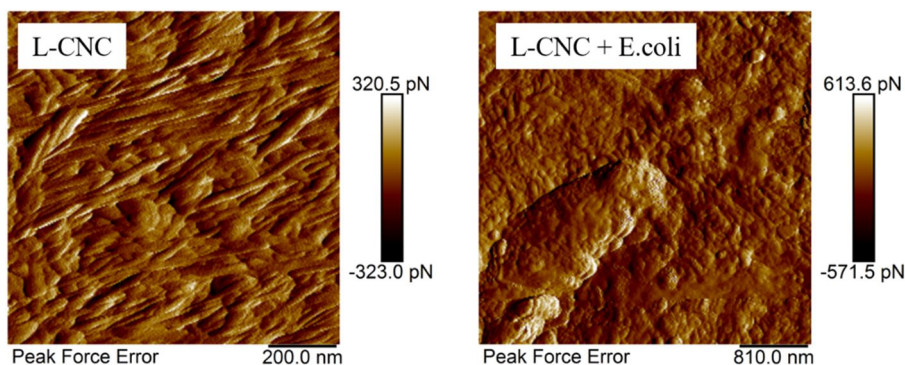


Figure 4.4 AFM peak force error images showing an L-CNC films that has not been exposed to bacteria, on the right, and *E. coli* on the surface of L-CNC film, on the left.

5. From lab-scale to pilot line: Scalability of coatings for commercialized PES membranes

During the last decade, the use of plant-derived nanocellulose for tailoring water-purification systems has been extensively studied and presented as a green-functionalized membrane solution on a laboratory scale, as the ones explained previously in this thesis. Nevertheless, most of the existing approaches based on renewable and bio-based materials suffer from a lack of efficient and scalable processing strategies. As our last goal for this thesis, we took the concepts developed in the laboratory and transferred them into a pilot line process.

Surface modification by layer-by-layer coatings in laboratory scale

In *paper I* we proposed a layer-by-layer deposition technique to modify membrane surfaces (see Figure 5.1). The method used the electrostatic interactions between the different components to bind them together. Electrostatically adsorbed modifiers deposited by layer-by-layer technique usually adhere robustly^{43,45}. Treating negatively charged PES membranes with the cationic polyelectrolyte PAHCl render the surface of the substrate positively charged and functioned as an anchoring layer for the negatively charged nanocellulose. The electrostatic interactions between the three layers guarantee a robust adhesion and a distinct stability of the coating.

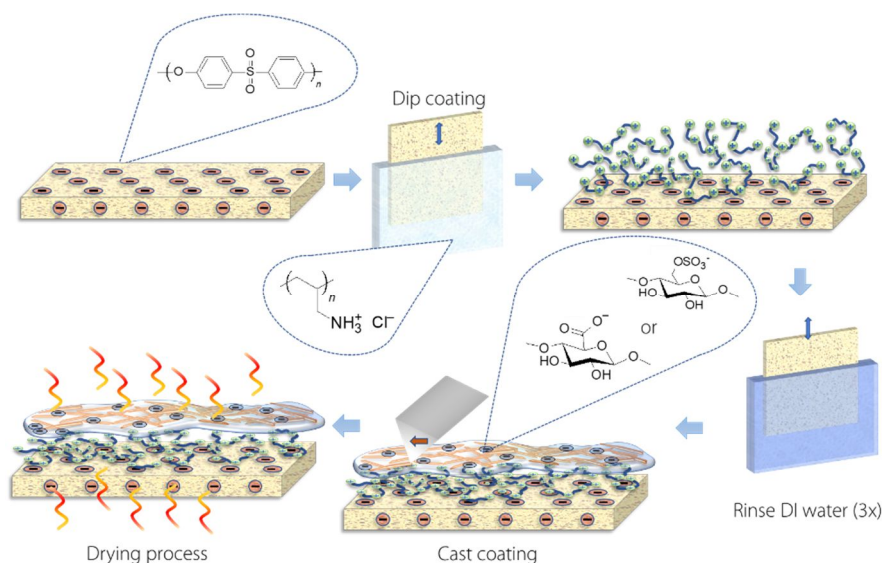


Figure 5.1 Conceptual schematic illustration of the layer-by-layer deposition process proposed in the laboratory scale. Taken from Aguilar-Sanchez et al.⁵⁶ and adapted with permission from Elsevier.

Surface modification in pilot line

In paper V, the knowledge gained from *papers I and II* was translated to a pilot-scale process, paving the way towards tunable and sustainable water-treatment technologies at an industrial level (Figure 5.2). First, the PES membrane was plasma-treated to hydrophilize the surface and assure the interfacial adhesion between the cationic b-PEI anchoring layer and the CNF. The b-PEI was added, then cast coating and spray coating were used to apply a thin layer of a nanocellulose mixture (CNF 75 wt%/ T-CNF 25 wt%) to PES membranes. The coating speed and thickness were optimized by studying the influence of the different process variables. In order to produce nanopolysaccharide-modified membranes suitable for the operational conditions in filtration processes (e.g. high pressure), the coating approach was chosen to produce interfacial adhesion and adequate wet strength during the process and final coated membrane. Finally, an acid-induced treatment was added after applying the coating to generate attractive interfibrillar interactions between CNF and T-CNF. Two different coating techniques, cast and spray coating, were tested to demonstrate the versatility of the coating formulation. Figure 5.2 presents a flow chart of the complete pilot line process.

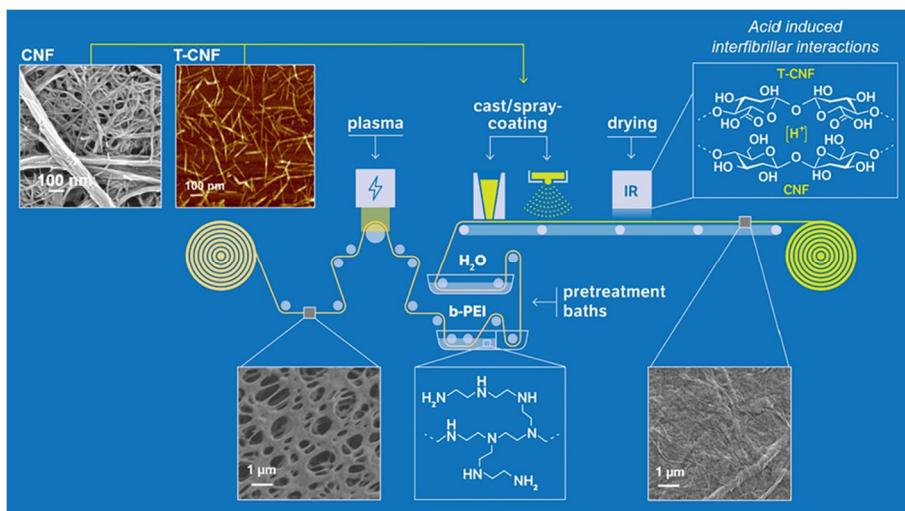


Figure 5.2 Cast/spray coating process flowchart at the pilot line. Taken from Pöhler et al.⁵³

Before scaling up the process, a QCM-D study was done to understand the strength of the interactions between the different components. It demonstrated that T-CNF did not spontaneously attach to PES surfaces, but that stable coatings could be achieved by using b-PEI as anchoring polymer, aligned with the concept presented in *paper I*. In addition, the PES–b-PEI–T-CNF layers remained stable after swelling in aqueous conditions. These results guided the upscaling of the process.

The membranes processed in the pilot line were characterized to understand the quality final properties and performance of the coatings. The coating thickness of the cast-coated membranes varied from an average of 600–800 nm, while for the spray-coated membranes it varied within 400–600 nm. AFM images revealed that all the coatings, were formed from a tight layer of T-CNF nanofibrils together with some coarser CNF nanofibers; and with lowered surface roughness compared to the pristine membrane. The coating layer evenness was demonstrated by comparing the sulfur and nitrogen percentages on the surface of the coated membranes. Sulfur could not be detected on the surface of the coated samples, meaning that the surface was evenly coated. The PES membrane substrate showed negative ζ -potential at neutral and high pH. With decreasing pH, the ζ -potential steadily increased towards isoelectricity and almost reached the isoelectric point at pH 2. Modifying the surface with b-PEI substantially changed the surface charge. The ζ -potential strongly increased with decreasing pH passing the isoelectric point at pH 7

and exhibiting positive surface charge at acidic pH. The cast-coated membranes with nanocellulose had significantly lower surface charge compared to the b-PEI modified substrate, confirming attachment of negatively charged nanocellulose. Below pH 9, the ζ -potential values of the coated membrane were more negative than the one of the b-PEI modified substrate and the isoelectric point was shifted to pH 4. For spray-coated membranes we observed the same effect, but with a slightly more positive ζ -potential compared to cast-coating. During spray coating the membrane surface, a more porous and/or uneven coating layer was attached to the membrane compared to castcoating, resulting in a stronger impact of b-PEI on the surface charge. In the case of hydrophilicity improvement, the coatings enhanced the surface wettability.

Regarding membrane filtration performance, the permeance of nanocellulose-coated membranes ranged between 100 to 200 LMH/MPa, which is significantly lower than the original permeance of microfiltration PES membrane (120 000 LMH/MPa at 0.25 MPa), in the range for ultrafiltration. All nanocellulose-coated membranes clearly rejected Cytochrome C, whereas zero rejection was attained for the uncoated MF PES membrane. Cast-coated membranes with an average coating thickness of 600 nm exhibited the highest rejection of >90%, while the thinnest spray coated membrane exhibited rejection at a lower level of approximately 70%, with relatively high variation attributed to irregularities in the coating structure. Various molecular weights and non-monodisperse but narrow MW distributions of anionic PSS and neutral dextrane molecules were used. In case of dextrane, the highest MWCO value at 90% rejection was ~14 000 Da for the spray-coated nanocellulose layer of ~420 nm. The cast-coated nanocellulose layers with a thickness of ~600 nm exhibited lower MWCO values of ~640 Da showing the large impact of the nanocellulose layer thickness on the MWCO. In case of anionic PSS, the spray coated sample with a layer thickness of ~420 nm yielded lower MWCO values of ~2000 Da compared to the ~14 000 Da measured for neutral dextrane. Hence, the negative surface charge of the nanocellulose coating induced charge-based rejection of the PSS molecules. In the case of thicker cast-coated nanocellulose layers of ~600 and ~840 nm, no significant difference was observed in MWCO probed with either charged PSS or neutral dextrans. Thus, surface charge had little impact once a critical nanocellulose layer thickness was exceeded and the rejection was predominantly governed by size-exclusion. Based on the MWCO investigation our nanocellulose-coated PES membranes are nanofiltration membranes (pore size 1–2 nm) close to the lower boundary of ultrafiltration membranes (pore size 2–100 nm).

Direct investigations on the fouling tendency of membrane materials were done by adsorbing a model protein, BSA, on PES, b-PEI, CNF and T-CNF surfaces. A significant mass uptake was detected on PES and b-PEI surfaces as indicated by a clear negative change in frequency. The adsorbed BSA formed a thin and rigid layer on PES and on b-PEI, indicating attractive interactions between the protein and the substrates. Contrary to these results, both nanocellulose grades were conferred antifouling properties on the PES membranes.

6. Summary and future work

Our research developed scalable bio-based nanopolysaccharide coatings for functional membranes and separation processes. We proposed three different coating-substrate approaches, which took advantage of the readily available substrates and improved their performance using nanocellulose and nanochitin to provide new functionality.

- Our first approach, simple layer-by-layer coating of CNC and T-CNF exhibited high improved antifouling performance, with up to 49% less relative adhesion of BSA compared to the PES uncoated membranes; in addition to modifying the selectivity, modifying the range from MF to UF regime.
- The second coating proposed was a robust chemically crosslinked 3-D network formed by PVA and T-CNF, which stabilized the nanocellulose layer and addressed the challenges faced by membranes used in an aqueous environment, including the mechanical properties of the membranes in wet conditions, and the stability of the coated layer during water flux and in a wide range of pH environments. In addition, the coating provided adsorption driven by electrostatic interaction, in addition to rejection due to size exclusion without significantly reducing the permeability, up to 75% less relative adhesion of BSA.
- A high-flux coating was proposed, in which fully bio-based membranes for water purification were developed, using CNC, T-CNF, and ChNC coatings to improve the wettability of the fabric and modified the surface charge. All of the systems showed excellent separation properties at a size of 500 nm, which makes them suitable for separating bacteria and some viruses. The T-CNF-modified fabrics collected the 2 μm particles and thus could be used to filter microplastics from water. The CNC- and T-CNF-impregnated fabrics showed antifouling capability against proteins at pH 7, while ChNC-impregnated fabrics performed well at acidic pH.

During our bacteria viability studies, we determined that T-CNF coated surfaces show outstanding antibacterial properties against *E. coli*, presumably due to the ability of carboxyl groups in T-CNF structure to lower the pH of the medium. T-CNF/PVA coatings showed a 0% of biofilm formation, which was assigned to the aldehyde groups present on the coated substrate.

Furthermore, non-woven cellulose fabrics impregnated with T-CNF and ChNC showed to be harmful to the bacteria colonizing.

Later comparison studies showed that exposure to different nanopolysaccharides affected bacteria proliferation to different extents. CNC did not show any bacterial-growth inhibition, while T-CNF had a cytostatic effect on *E. coli*. AFM studies revealed that there was bacterial damage when the *E. coli* was in direct contact with L-CNC, T-CNF, or ChNC. This was demonstrated by imaging, changes in roughness, DMT modulus, and adhesion forces. Nevertheless, CNC films seemed to serve as a carbon source for the *E. coli* cells to grow and proliferate.

Lastly, we demonstrated the feasibility of using nanocellulose in a pilot-scale cast- and spray-coating process to modify polymeric PES microfiltration membranes. Formulations proposed throughout this thesis are likely to be easily scalable due to the limited modification that is required for industrial manufacturing lines.

As for the future, we consider it necessary to continue studying the effect of nanopolysaccharides over bacterial viability to perform biological studies in static conditions, to complement the AFM study. Likewise, a study with gram-positive bacteria would be useful to compare to our current gram-negative results and generate further understanding of the interactions.

In conclusion, we foresee that the fundamental understanding and concepts applied for the developed coating proposals exposed in this thesis can be extrapolated to other types of polymeric surfaces and applications.

7. Acknowledgements

I will start by thanking the European Union's Horizon 2020 research and innovation program (grant agreement No 760601) for providing the funding for my research. Also, I want to express my sincerest gratitude to my supervisor Prof. Aji P. Mathew for giving me such a life-changing opportunity to pursue my Ph.D. studies in your group. It is really valuable to have a warm-hearted person as a supervisor! Also, thanks to all the collaborators from the Nanotext Surf project. It was nice working with you during the last 4 years! Overall, thanks to all MMK staff with whom I shared moments and who helped me along the way, I admire you all! It has been a pleasure to be surrounded by such smart and hard-working people who inspire me every day. These are the things that make working-life special. Thanks to my research group colleagues for fruitful discussions and collaborations. I will miss you! Thanks to Jakob for all the help along the years with the weird experimental set-ups needed along the way. Thanks to Tamara, Laura P., Natalia, Vera, and Blanca for the support while writing this thesis. To my old and current officemates: Blanca (again), thanks for your guidance during the first years, and sharing your passion for microbiology and living microorganisms, and of course for your friendship! Dimi, my Ph.D. twin, it was amazing sharing this ride with you, both during the ups and downs. I can't imagine going through all of this without you. Natalia (again), girl, I remember your excitement when I first met you. Don't allow anything to steal that glow in your eyes. Thanks for being such an amazing friend/colleague/neighbor! To my Latin-American colleagues/friends/family at MMK, Luis, Ximena, and Ilse thank you for making easier all the cultural shocks and helping me forget that I am living far away from home. You are amazing friends (like the ones you can only get on our side of the world). I admire you every single day! To the Persian girls, Atefeh, Sadaf, and Elnaz, you are so smart and sweet! I need to go to Iran since it seems to be a place with amazing people like you! To all the "fifth-floorers" that I have shared summer trips and beers with, you are amazing people! It is a shame that you are not on the fourth floor :P. To my gang of Ticos in Stockholm, Mau, Carlos, and Yani, thanks for giving me the feeling of Costa Rica in the middle of Scandinavia. You made easier the long periods without going back home. To my Anchor boys (Luis and Dimi again, Andreas and Iosif), thanks for making me feel like the most beautiful girl in the group :P, and for your caring friendship, trips, and beers (and shots of course). To Luisca, thanks for all the journeys, including this! To Laura S., thanks for being my life-saver during the Ph.D., there is no way I would have been able to do it without you! To Martin, thanks for your enormous patience towards

me during these crazy times, for your big heart and sweetness! To Bongo, my old puppy, for giving me rest when I felt restless and making me smile just by being around me. To Kika, to whom this thesis is dedicated, you are present in my life every single day! Thank you for giving me the honor of spending your last weeks on Earth with me. You gave me countless laughs, wise advice, and love. To my mother, there are no words to describe my gratitude towards you, I wouldn't be anything without your love. And to life, for giving me all the previously mentioned people as a companion along the way.

8. References

- (1) Nations, U. Sustainable development goals
<https://www.un.org/sustainabledevelopment/>.
- (2) Voisin, H.; Bergström, L.; Liu, P.; Mathew, A. P. Nanocellulose Based Materials for Water Purification. *nanomaterials* **2017**, 7 (3), 1–18.
- (3) Zhang, D.; Karkooti, A.; Liu, L.; Sadrzadeh, M.; Thundat, T.; Liu, Y.; Narain, R. Fabrication of Antifouling and Antibacterial Polyethersulfone (PES) /Cellulose Nanocrystals (CNC) Nanocomposite Membranes. *J. Memb. Sci.* **2018**, 549, 350–356.
- (4) Valencia, L.; Arumughan, V.; Jalvo, B.; Maria, H. J.; Thomas, S.; Mathew, A. P. Nanolignocellulose Extracted from Environmentally Undesired Prosopis Juliflora. *ACS OMEGA* **2019**, 4, 4330–4338.
- (5) Lv, J.; Zhang, G.; Zhang, H.; Zhao, C.; Yang, F. Improvement of Antifouling Performances for Modified PVDF Ultrafiltration Membrane with Hydrophilic Cellulose Nanocrystal. *Appl. Surf. Sci.* **2018**, 440, 1091–1100.
- (6) Georgouvelas, D.; Jalvo, B.; Valencia, L.; Papawassiliou, W.; Pell, A. J.; Edlund, U.; Mathew, A. P. Residual Lignin and Zwitterionic Polymer Grafts on Cellulose Nanocrystals for Antifouling and Antibacterial Applications. *ACS Appl. Polym. Mater.* **2020**, No. 2, 3060–3071.
- (7) Ma, H.; Chu, B.; Hsiao, B. S. Functional Nanofibers for Water Purification. In *Functional Nanofibers and their Applications*; Wei, Q., Ed.; Woodhead Publishing, 2012; pp 331–370.
- (8) Qin, A.; Li, X.; Zhao, X.; Liu, D.; He, C. Preparation and Characterization of Nano-Chitin Whisker Reinforced PVDF Membrane with Excellent Antifouling Property. *J. Memb. Sci.* **2015**, 480, 1–10. <https://doi.org/10.1016/j.memsci.2015.01.035>.
- (9) Naseri, N.; Mathew, A. P.; Girandon, L.; Fröhlich, M.; Oksman, K. Porous Electrospun Nanocomposite Mats Based on Chitosan–Cellulose Nanocrystals for Wound Dressing: Effect of Surface Characteristics of Nanocrystals. *Cellulose* **2015**, 22 (1), 521–534. <https://doi.org/10.1007/s10570-014-0493-y>.
- (10) Mera, A.; Araki, J.; Ohtsuki, T. Chitin Nanowhiskers Mediate Transformation of Escherichia Coli by Exogenous Plasmid DNA. *J. Biotechnol. Biomater.* **2011**, 01 (06), 1–6.

<https://doi.org/10.4172/2155-952x.1000114>.

- (11) Daraei, P.; Ghaemi, N.; Sadeghi Ghari, H. An Ultra-Antifouling Polyethersulfone Membrane Embedded with Cellulose Nanocrystals for Improved Dye and Salt Removal from Water. *Cellulose* **2017**, *24*, 915–929.
- (12) Ma, H.; Burger, C.; Hsiao, B. S.; Chu. Ultrafine Polysaccharide Nanofibrous Membranes for Water Purification. *Biomacromolecules* **2011**, *12* (4), 970–976.
- (13) Goetz, L. A.; Jalvo, B.; Rosal, R.; Mathew, A. P. Superhydrophilic Anti-Fouling Electrospun Cellulose Acetate Membranes Coated with Chitin Nanocrystals for Water Filtration. *J. Memb. Sci.* **2016**, *510*, 238–248.
- (14) Goetz, L. A.; Naseri, N.; Nair, S. S.; Karim, Z.; Mathew, A. P. All Cellulose Electrospun Water Purification Membranes Nanotextured Using Cellulose Nanocrystals. *Cellulose* **2018**, *25*, 3011–3023.
- (15) Karim, Z.; Mathew, A. P.; Kokol, V.; Wei, J.; Grahn, M. High-Flux Affinity Membranes Based on Cellulose Nanocomposites for Removal of Heavy Metal Ions from Industrial Effluents. *RCS Adv.* **2016**, *6*, 20644–20653.
- (16) Georgouvelas, D.; Abdelhamid, H. N.; Li, J.; Edlund, U.; Mathew, A. P. All-Cellulose Functional Membranes for Water Treatment: Adsorption of Metal Ions and Catalytic Decolorization of Dyes. *Carbohydr. Polym.* **2021**, *264* (January), 118044. <https://doi.org/10.1016/j.carbpol.2021.118044>.
- (17) Liu, P.; Oksman, K.; Mathew, A. P. Surface Adsorption and Self-Assembly of Cu(II) Ions on TEMPO-Oxidized Cellulose Nanofibers in Aqueous Media. *J. Colloid Interface Sci.* **2016**, *464*, 175–182.
- (18) Karim, Z.; Claudpierre, S.; Grahn, M.; Oksman, K.; Mathew, A. P. Nanocellulose Based Functional Membranes for Water Cleaning: Tailoring of Mechanical Properties, Porosity and Metal Ion Capture. *J. Memb. Sci.* **2016**, *514*, 418–428.
- (19) Sharma, P. R.; Sharma, S. K.; Lindström, T.; Hsiao, B. S. Nanocellulose-Enable Membranes for Water Purification: Perspectives. *Adv. Sustain. Syst.* **2020**, *4*, 1900114.
- (20) Mays, T. J. A New Classification of Pore Sizes. *Stud. Surf. Sci. Catal.* **2007**, *160* (Characterization of Porous Solids VII), 57–62.
- (21) Hamid, S. A.; Azha, S. F.; Sellaoui, L.; Bonilla-Petriciolet, A.;

- Ismail, S. Adsorption of Copper (II) Cation on Polysulfone/Zeolite Blend Sheet Membrane: Synthesis, Characterization, Experiments and Adsorption Modelling. *Colloids Surfaces A* **2020**, *601*, 124980.
- (22) Breite, D.; Went, M.; Prager, A.; Kuehnert, M.; Schulze, A. Charge Separating Microfiltration Membrane with PH-Dependent Selectivity. *Polymers (Basel)*. **2019**, *11*, 3.
 - (23) Liu, P.; Sehaqui, H.; Tingaut, P.; Wichser, A.; Oksman, K.; Mathew, A. P. Cellulose and Chitin Nanomaterials for Capturing Silver Ions (Ag⁺) from Water via Surface Adsorption. *Cellulose* **2014**, *21* (1), 449–461. <https://doi.org/10.1007/s10570-013-0139-5>.
 - (24) Miller, D. J.; Dreyer, D. R.; Bielawski, C. W.; Paul, D. R.; Freeman, B. D. Surface Modification of Water Purification Membranes: A Review. *Angew. Chemie* **2017**, *56* (17), 4662–4711.
 - (25) Singh, J.; Shrivastava, A.; Mukophadhyaya, K.; Prasad, D.; Sharma, V. Design and Development of Composite Nonwoven Filter for Pre-Filtration of Textile Effluents Using Nano-Technology. *J. Mater. Sci. Eng.* **2017**, *6* (3). <https://doi.org/10.4172/2169-0022.1000340>.
 - (26) Peniche, C.; Arguelles-Monal, W.; Goycoolea, M. Chitin and Chitosan : Major Sources, Properties and Applications. In *Monomers, Polymers and Composites from Renewable Resources*; Belgacem, M. N., Gandini, A., Eds.; Elsevier, 2008; pp 517–542.
 - (27) Song, F.; Koo, H.; Ren, D. Effects of Material Properties on Bacterial Adhesion and Biofilm Formation. *J. Dent. Res.* **2015**, *94* (8), 1027–1034. <https://doi.org/10.1177/0022034515587690>.
 - (28) Katsikogianni, M.; Missirlis, Y. F.; Harris, L.; Douglas, J. Concise Review of Mechanisms of Bacterial Adhesion to Biomaterials and of Techniques Used in Estimating Bacteria-Material Interactions. *Eur. Cells Mater.* **2004**, *8*, 37–57. <https://doi.org/10.22203/eCM.v008a05>.
 - (29) O'Toole, G.; Kaplan, H. B.; Kolter, R. Biofilm Formation as Microbial Development. *Annu. Rev. Microbiol.* **2000**, *54*, 49–79.
 - (30) Lasa, I. Towards the Identification of the Common Features of Bacterial Biofilm Development. *Int. Microbiol.* **2006**, *9* (1), 21–28. <https://doi.org/10.2436/im.v9i1.9545>.
 - (31) Marshall, A. D.; Munro, P. A.; Trägårdh, G. The Effect of Protein Fouling in Microfiltration and Ultrafiltration on Permeate Flux, Protein Retention and Selectivity: A Literature Review. *Desalination* **1993**, *91*, 65–108.

- (32) Belfort, G.; Davis, R. H.; Zydney, A. L. The Behavior of Suspensions and Macromolecular Solutions in Crossflow Microfiltration. *J. Memb. Sci.* **1994**, *96*, 1–58.
- (33) Ridgway, H. F.; Rigby, M. G.; Argo, D. G. Bacterial Adhesion and Fouling of Reverse Osmosis Membranes. *J. Am. Water Work. Assoc.* **1985**, *77*, 97–106.
- (34) Flemming, H.-C.; Schaule, G.; Griebe, T.; Schmitt, J.; Tamachkiarowa, A. Biofouling-the Achilles Heel of Membrane Processes. *Desalination* **1997**, *113*, 215–225.
- (35) Herzberg, M.; Kang, S.; Elimelech, M. Role of Extracellular Polymeric Substances (EPS) in Biofouling of Reverse Osmosis Membranes. *Environ. Sci. Technol.* **2009**, *43* (12), 4393–4398.
- (36) Hall-Stoodley, L.; Costerton, J. W.; Stoodley, P. Bacterial Biofilms: From the Natural Environment to Infectious Diseases. *Nat. Rev. Microbiol.* **2004**, *2* (2), 95–108. <https://doi.org/10.1038/nrmicro821>.
- (37) Ma, H.; Burger, C.; Hsiao, B. S.; Chu, B. Fabrication and Characterization of Cellulose Nanofiber Based Thin-Film Nanofibrous Composite Membranes. *J. Memb. Sci.* **2014**, *454*, 272–282. <https://doi.org/10.1016/j.memsci.2013.11.055>.
- (38) Campoccia, D.; Montanaro, L.; Arciola, C. R. A Review of the Biomaterials Technologies for Infection-Resistant Surfaces. *Biomaterials* **2013**, *34*, 8533–8554.
- (39) Chen, S.; Li, L.; Zhao, C.; Zheng, J. Surface Hydration: Principles and Applications toward Low-Fouling/Nonfouling Biomaterials. *Polymer (Guildf)*. **2010**, *51* (23), 5283–5293.
- (40) Pogodin, S.; Hasan, J.; Baulin, V. A.; Webb, H. K.; Truong, V. K.; Nguyen, T. H. P.; Boshkpvikj, V.; Fluke, C. J.; Watson, G. S.; Watson, J. A.; Crawford, R. J.; Ivanova, E. P. Biophysical Model of Bacterial Cell Interactions with Nanopatterned Cicada Wing Surfaces. *Biophys. J.* **2013**, *104*, 835–840.
- (41) Platypus Technologies, L. <https://www.platypustech.com/>
<https://www.platypustech.com/wp-content/uploads/hydrophobic-hydrophilic-surface-1.jpg>.
- (42) Aggarwal, S.; Koser, K.; Chakravarty, A.; Ikram, S. Understanding How the Substituents of Polysaccharides Influence Physical Properties. In *Innovation in nanopolysaccharides for eco-sustainability: From Science to Industrial Applications*; 2022; pp 119–132.

- (43) Mautner, A.; Lee, K.-Y.; Lahtinen, P.; Hakalahti, M.; Tammelin, T.; Li, K.; Bismarck, A. Nanopapers for Organic Solvent Nanofiltration. *ChemComm* **2014**, *50*, 5778–5781.
- (44) Mautner, A.; Lee, K.-Y.; Lahtinen, P.; Hakalahti, M.; Tammelin, T.; Li, K.; Bismarck, A. Nanopapers for Organic Solvent Nanofiltration. *Chem. Commun.* **2014**, *50*, 5778–5781.
- (45) Mautner, A.; Lee, K.-Y.; Tammelin, T.; Mathew, A. P.; Nedoma, A. J.; Li, K.; Bismarck, A. Cellulose Nanopapers as Tight Aqueous Ultra-Filtration Membranes. *React. Funct. Polym.* **2015**, *86*, 209–214.
- (46) Doherty, W. O. S.; Mousavioun, P.; Fellows, C. M. Value-Adding to Cellulosic Ethanol: Lignin Polymers. *Ind. Crops Prod.* **2011**, *33*, 259–276.
- (47) Habibi, Y.; Lucia, L. A.; Rojas, O. J. Cellulose Nanocrystals: Chemistry, Self-Assembly and Applications. *Chem. Rev.* **2010**, *110* (6), 3479–3500.
- (48) Saito, T.; Hirota, M.; Tamura, N.; Kimura, S.; Fukuzumi, H.; Heux, L.; Isogai, A. Individualization of Nano-Sized Plant Cellulose Fibrils by Direct Surface Carboxylation Using TEMPO Catalyst under Neutra Conditions. *Biomacromolecules* **2009**, *10* (7), 1992–1996.
- (49) Jalvo, B.; Mathew, A. P.; Rosal, R. Coaxial Poly(Lactic Acid) Electrospun Composite Membranes Incorporating Cellulose and Chitin Nanocrystals. *J. Memb. Sci.* **2017**, *544*, 261–271.
- (50) Moreno, A.; Liu, J.; Morsali, M.; Sipponen, M. H. Chemical Modification and Functionalization of Lignin Nanoparticles. In *Micro and Nanolignin in Aqueous Dispersions and Polymers*; Elsevier, 2022; pp 385–431.
- (51) Kaya, M.; Mujtaba, M.; Ehrlich, H.; Salaberria, A. M.; Baran, T.; Amemiya, C. T.; Galli, R.; Akyuz, L.; Sargin, I.; Labidi, J. On Chemistry of γ -Chitin. *Carbohydr. Polym.* **2017**, *176* (August), 177–186. <https://doi.org/10.1016/j.carbpol.2017.08.076>.
- (52) Isogai, A.; Saito, T.; Fukuzumi, H. TEMPO-Oxidized Cellulose Nanofibers. *Nanoscale* **2011**, *3*, 71.
- (53) Pöhler, T.; Mautner, A.; Aguilar-Sanchez, A.; Hansmann, B.; Kunnari, V.; Grönroos, A.; Rissanen, V.; Siqueira, G.; Mathew, A. P.; Tammelin, T. Pilot-Scale Modification of Polyethersulfone Membrane with a Size and Charge Selective Nanocellulose Layer. *Sep. Purif. Technol.* **2022**, *285*, 120341.

- (54) Jalvo, B.; Aguilar-Sanchez, A.; Ruiz-Caldas, M.-X.; Mathew, A. P. Water Filtration Membranes Based on Non-Woven Cellulose Fabrics: Effect of Nanopolysaccharide Coatings on Selective Particle Rejection, Antifouling, and Antibacterial Properties. *nanomaterials* **2021**, *11*, 1752.
- (55) Ali, S. W.; Rajendran, S.; Joshi, M. Effect of Process Parameters on Layer-by-Layer Self-Assembly of Polyelectrolytes on Cotton Substrate. *Polym. Polym. Compos.* **2010**, 237–249.
- (56) Aguilar-Sanchez, A.; Jalvo, B.; Mautner, A.; Nameer, S.; Pöhler, T.; Tammelin, T.; Mathew, A. P. Waterborne Nanocellulose Coatings for Improving the Antifouling and Antibacterial Properties of Polyethersulfone Membranes. *J. Memb. Sci.* **2021**, *620*, 118842.
- (57) Aguilar-Sanchez, A.; Jalvo, B.; Mautner, A.; Rissanen, V.; Kontturi, K. S.; Abdelhamid, H. N.; Tammelin, T.; Mathew, A. P. Charged Ultrafiltration Membranes Based on TEMPO-Oxidized Cellulose Nanofibrils/Poly(Vinyl Alcohol) Antifouling Coating. *RSC Adv.* **2021**, *11*, 6859–6868.
- (58) Zhang, R.; Liu, Y.; He, M.; Su, Y.; Zhao, X.; Elimelech, M.; Jiang, Z. Antifouling Membranes for Sustainable Water Purification Strategies and Mechanisms. *Chem. Soc. Rev.* **2016**, *45* (21), 5888–5924.
- (59) Zhang, C.; Wei, K.; Zhang, W.; Bai, Y.; Sun, Y.; Gu, J. Graphene Oxide Quantum Dots Incorporated into a Thin Film Nanocomposite Membrane With High Flux and Antifouling Properties for Low-Pressure Nanofiltration. *ACS Appl. Mater. Interfaces* **2017**, *9*, 11082–11094.
- (60) Zhao, S.; Wang, Z.; Wei, X.; Zhao, B.; Wang, J.; Yang, S.; Wang, S. Performance Improvement of Polysulfone Ultrafiltration Membrane Using Well-Dispersed Polyaniline-Poly(Vinylpyrrolidone) Nanocomposite as the Additive. *Ind. Eng. Chem. Res.* **2012**, *51*, 4661–4672.
- (61) Hakalahti, M.; Salminen, A.; Seppälä, J.; Tammelin, T.; Hänninen, T. Effect of Interfibrillar PVA Bridging on Water Stability and Mechanical Properties of TEMPO/NaClO₂ Oxidized Cellulosic Nanofibril Films. *Carbohydr. Polym.* **2015**, *126*, 78–82.
- (62) Kim, K.-J.; Lee, S.-B.; Han, N.-W. Effect of the Degree of Crosslinking on Properties of Poly(Vinyl Alcohol) Membranes. *Polym. J.* **1993**, *25* (12), 1295–1302.

- (63) Kozlov, M.; Quarmyne, M.; Che, W.; McCarthy, T. J. Adsorption of Poly(Vinyl Alcohol) onto Hydrophobic Substrates. A General Approach for Hydrophilizing and Chemically Activating Surfaces. *Macromolecules* **2003**, *36*, 6054–6059.
- (64) Ma, X.; Su, Y.; Sun, Q.; Wang, Y.; Jiang, Z. Enhancing the Antifouling Property of Polyethersulfone Ultrafiltration Membranes through Surface Adsorption-Crosslinking of Poly(Vinyl Alcohol). *J. Memb. Sci.* **2007**, *300*, 71–78.
- (65) Hou, T.; Guo, K.; Wang, Z.; Zhang, X.-F.; Feng, Y.; He, M.; Yao, J. Glutaraldehyde and Polyvinyl Alcohol Crosslinked Cellulose Membranes for Efficient Methyl Orange and Congo Red Removal. *Cellulose* **2019**, *26*, 5065–5074.
- (66) Tang, C.; Saquing, C. D.; Harding, J. R.; Khan, S. A. In Situ Cross-Linking of Electrospun Poly(Vinyl Alcohol) Nanofibers. *Macromolecules* **2010**, *43*, 630–637.
- (67) Kim, K.-J.; Lee, S.-B.; Han, N.-W. Kinetics of Crosslinking Reaction of PVA Membrane with Glutaraldehyde. *Korean J. Chem. Eng.* **1994**, *11* (1), 41–47.
- (68) Yeom, C.-K.; Lee, K.-H. Pervaporation Separation of Water-Acetic Acid Mixtures through Poly(Vinyl Alcohol) Membranes Crosslinked with Glutaraldehyde. *J. Memb. Sci.* **1996**, *109*, 257–265.
- (69) Praptowidodo, V. S. Influence of Swelling on Water Transport through PVA-Based Membrane. *J. Mol. Struct.* **2005**, *739*, 207–212.
- (70) Stewart, M.; Arnold, K. Water Injection Systems. In *Emulsions and Oil Treating Equipment*; Stewart, M., Arnold, K., Eds.; Gulf Professional Publishing, 2009; pp 213–265.
<https://doi.org/10.1016/b978-0-7506-8970-0.00004-9>.
- (71) Phan, H. T. M.; Bartelt-Hunt, S.; Rodenhausen, K. B.; Schubert, M.; Bartz, J. C. Investigation of Bovine Serum Albumin (BSA) Attachment onto Self-Assembled Monolayers (SAMs) Using Combinatorial Quartz Crystal Microbalance with Dissipation (QCM-D) and Spectroscopic Ellipsometry (SE). *PLoS One* **2015**, *10* (10).
<https://doi.org/10.1371/journal.pone.0141282>.
- (72) Shirahama, H.; Takeda, K.; Suzawa, T. Adsorption of Bovine Serum Albumin onto Polystyrene Latex: Effects of Coexistent Electrolyte Anions. *J. Colloid Interface Sci.* **1986**, *109* (2), 552–556.
[https://doi.org/10.1016/0021-9797\(86\)90336-X](https://doi.org/10.1016/0021-9797(86)90336-X).
- (73) Hughes Wassell, D. T.; Embery, G. Adsorption of Bovine Serum

- Albumin on to Titanium Powder. *Biomaterials* **1996**, *17* (9), 859–864. [https://doi.org/10.1016/0142-9612\(96\)83280-7](https://doi.org/10.1016/0142-9612(96)83280-7).
- (74) Kudelski, A. Influence of Electrostatically Bound Proteins on the Structure of Linkage Monolayers: Adsorption of Bovine Serum Albumin on Silver and Gold Substrates Coated with Monolayers of 2-Mercaptoethanesulphonate. *Vib. Spectrosc.* **2003**, *33* (1–2), 197–204. <https://doi.org/10.1016/j.vibspec.2003.09.003>.
 - (75) Bajpai, A. K. Adsorption of Bovine Serum Albumin onto Glass Powder Surfaces Coated with Polyvinyl Alcohol. *J. Appl. Polym. Sci.* **2000**, *78* (5), 933–940. [https://doi.org/10.1002/1097-4628\(20001031\)78:5<933::AID-APP10>3.0.CO;2-G](https://doi.org/10.1002/1097-4628(20001031)78:5<933::AID-APP10>3.0.CO;2-G).
 - (76) Kopac, T.; Bozgeyik, K.; Yener, J. Effect of PH and Temperature on the Adsorption of Bovine Serum Albumin onto Titanium Dioxide. *Colloids Surfaces A Physicochem. Eng. Asp.* **2008**, *322* (1–3), 19–28. <https://doi.org/10.1016/j.colsurfa.2008.02.010>.
 - (77) Servagent-Noinville, S.; Revault, M.; Quiquampoix, H.; Baron, M. H. Conformational Changes of Bovine Serum Albumin Induced by Adsorption on Different Clay Surfaces: FTIR Analysis. *J. Colloid Interface Sci.* **2000**, *221* (2), 273–283. <https://doi.org/10.1006/jcis.1999.6576>.
 - (78) Lynd, L. R.; Weimer, P. J.; van Zyl, W. H.; Pretorius, I. S. Microbial Cellulose Utilization: Fundamentals and Biotechnology. *Microbiology Mol. Biol. Rev.* **2002**, *66* (3), 506–577.
 - (79) Atsumi, S.; Liao, J. C. Metabolic Engineering for Advanced Biofuels Production from Escherichia Coli. *Curr. Opin. Biotechnol.* **2008**, *19* (5), 414–419.
 - (80) Pang, J.; Liu, Z.-Y.; Hao, M.; Zhang, Y.-F.; Qi, Q.-S. An Isolated Cellulolytic Escherichia Coli from Bovine Rumen Produces Ethanol and Hydrogen from Corn Straw. *Biotechnol. Biofuels* **2017**, *10* (165).
 - (81) Dineen, P. Antibacterial Activity of Oxidized Regenerated Cellulose. *Surg. Gynecol. Obstet.* **1976**, *142* (4), 481–486.
 - (82) Atlas, R. M.; Bartha, R. *Microbial Ecology: Fundamentals and Applications*, 4th ed.; Addison Wesley Longman Publish, 1981.
 - (83) Kostenbauder, H. Physical Factors Influencing the Activity of Antimicrobial Agents. In *Desinfection, sterilization and preservation*; Block, S., Ed.; Lea & Febiger: Philadelphia, 1991; pp 59–71.
 - (84) Renner, L. D.; Weibel, D. B. Physicochemical Regulation of Biofilm

Formation. *MRS Bull.* **2011**, 36 (5), 347–355.

- (85) Teughels, W.; Van Assche, N.; Sliepen, I.; Quirynen, M. Effect of Material Characteristics and/or Surface Topography on Biofilm Development. *Clin. Oral Implants Res.* **2006**, 17 (52), 68–81.
- (86) Ong, Y. L.; Razatos, A.; Georgiou, G.; Sharma, M. M. Adhesion Forces between E. Coli Bacteria and Biomaterial Surfaces. *Langmuir* **1999**, 15 (8), 2719–2725. <https://doi.org/10.1021/la981104e>.
- (87) Zi, Y.; Zhu, M.; Li, X.; Xu, Y.; Wei, H.; Li, D.; Mu, C. Effects of Carboxyl and Aldehyde Groups on the Antibacterial Activity of Oxidized Amylose. *Carbohydr. Polym.* **2018**, 192, 118–125.
- (88) Andres, Y.; Giraud, L.; Gerente, C.; Le Cloirec, P. Antibacterial Effects of Chitosan Powder: Mechanisms of Action. *Environ. Technol.* **2007**, 28 (12), 1357–1363. <https://doi.org/10.1080/09593332808618893>.
- (89) Miklasinska-Majdanik, M.; Kepa, M.; Wojtyczka, R. D.; Idzik, D.; Wasik, T. J. Phenolic Compounds Diminish Antibiotic Resistance of Staphylococcus Aureus Clinical Strains. *Int. J. Environ. Res. Public Health* **2018**, 15, 2321.
- (90) Liu, Q.; Wu, J.; Lim, Z. Y.; Aggarwal, A.; Yang, H.; Wang, S. Evaluation of the Metabolic Response of Escherichia Coli to Electrolysed Water by ¹H NMR Spectroscopy. *LWT-Food Sci. Technol.* **2017**, 79, 428–436. <https://doi.org/10.1016/j.lwt.2017.01.066>.